Performance Analysis of Membrane Based Air-to-Air Enthalpy Recovery Units

Abdul Manan
Alireza Afshari
Niels C. Bergsøe

SBi
Danish Building Research Institute, Aalborg University Copenhagen· 2018

Title	Performance Analysis of Membrane Based Air-to-Air Enthalpy Recovery Units
Serial title	
Edition	1 edition
Year	2018
Author	Abdul Manan, Alireza Afshari, Niels C. Bergsøe
Language	English
Pages	52
References	51
Danish summary	4
ISBN	
ISSN	
Drawings	Abdul Manan
Photos	Abdul Manan
Publisher	SBi, Statens Byggeforskningsinstitut, Aalborg Universitet, Danish Building Research Institute, Aalborg University A.C. Meyers Vænge 15, 2450 Copenhagen SV E-mail sbi@sbi.aau.dk www.sbi.dk

Summary

Improvement in the energy saving performance in the ventilation system and to ensure a satisfactory indoor climate has been a challenging task in Denmark as well as in other cold countries. Usually rotary wheels enthalpy exchangers are used in energy recovery ventilation system. These exchangers recuperate above 80 % enthalpy energy. However, cross contamination, ice formation, size, and extra motor for operation are the drawbacks of using the rotary wheels. Therefore, it was relevant to study the performance of rather new air-to-air enthalpy exchangers under cold climate. These exchangers were stationary and no extra motor was required for the operation. Short-term performance analyses of air-to-air enthalpy exchangers can be found in the literature but long-term performance analyses has not been done yet for all I know. There was also deficiency of the knowledge regarding ice formation in the membranes, deformation in the membranes and gas transfer through the membranes.

In the present research project, performance of one air-to-air heat and four air-to-air enthalpy exchangers was analysed in terms of energy saving potential, ice accretion on the surface of the membranes and deformation in the membranes of the enthalpy exchangers. Performance was also analysed in terms of gas transfer through polymer and paper membranes of enthalpy exchangers. A test rig was built for laboratory tests and experiments were conducted at different outdoor air temperatures and airflows in order to analyse short and long-term performance.

The results show that the polymer membrane based enthalpy exchanger recuperated enthalpy energy 15 % more than treated paper membrane and 32 % more than paper membrane based enthalpy exchanger. About 79 % total energy was recuperated using polymer membrane based enthalpy exchanger. The ratio of the amount of latent energy transferred by the polymer membrane based enthalpy exchanger was 5 % to 12 % of the total energy, which is usually wasted in the sensible heat exchanger.

The outdoor air temperature had no influence on sensible effectiveness. However, latent effectiveness increased 3 % - 4 % and the total effectiveness decreased 7 % - 9 % with the increase in the outdoor air temperature from -16 ºC to 5 ºC.

Sensible, latent and total effectiveness were functions of face velocity. There was inverse relation between face velocity and the effectiveness.

No visible ice accretion and deformation in the paper, treated paper and polymer membranes was observed during short term and long-term studies.

There was no influence of outdoor air temperature and concentration of the gas on the transfer ratio through the paper and polymer membranes. The ratio of the amount of N_2O gas transferred through polymer membrane and treated paper membrane was 5 % and 13 % respectively.

Sammenfatning

Forøgelse af energibesparelsen i ventilationssystemer og sikring af et tilfredsstillende indeklima er en udfordrende opgave både i Danmark og i andre lande med såkaldt koldt klima. Normalt anvendes roterende genvindere med en entalpivirkningsgrad på over 80 %. Krydskontaminering, isdannelse, den fysiske størrelse og en ekstra motor til drift af rotoren er imidlertid ulemper ved at anvende roterende genvindere. Det var derfor relevant at studere ydeevnen af forholdsvis nye luft-til-luft membranbaserede entalpigenvindere. Sådanne genvindere er stationære og en ekstra motor er ikke nødvendig for driften. I litteraturen findes analyser af korttidsydeevnen af luft-til-luft entalpigenvindere, hvorimod der ikke er fundet eksempler på analyser af langtidsydeevnen. Der er derudover mangel på viden om risikoen for isdannelse i membranen, deformation af membranen og luftoverføring gennem membranen.

I det foreliggende forskningsprojekt blev resultater undersøgelser af en luft-til-luft varmegenvinder og fire luft-til-luft membranbaserede entalpigenvindere analyseret med hensyn til energibesparelsespotentiale, isdannelse på membranens overflade og deformation af membranen. Ydeevnen blev desuden analyseret i form af luftoverføring gennem polymer- og papirmembraner. Der blev opbygget en forsøgsopstilling, og undersøgelser blev udført ved forskellige udetemperaturer og ved forskellige luftstrømme for at analysere korttids- og langtidsydeevne.

Resultaterne viser, at entalpigenvinderen med polymermembran havde en entalpivirkningsgrad, som var 15 % større end genvinderen med en membran baseret på behandlet papir og 32 % større end genvinderen med papirmembran. Omkring 79 % totalenergi blev genvundet ved anvendelse af polymermembranen. Forholdet mellem mængden af latent energi overført i entalpigenvinderen med polymermembran var 5-12 % af den samlede energi, som går tabt i typiske kryds- og modstrømsvarmegenvindere.

Udetemperaturen havde ingen indflydelse på den sensible virkningsgrad, hvorimod den latente virkningsgrad steg med 3-4 %, og den totale virkningsgrad faldt med 7-9 % ved en stigning i udetemperatur fra -16 ° C til 5 ° C.

Sensibel, latent og totalvirkningsgrad blev fundet til at være funktioner af lufthastigheden over membranen, og der blev fundet en omvendt relation mellem lufthastigheden over membranen og virkningsgraden.

Der blev ikke observeret synlig isdannelse og ej heller deformation af membranen – såvel papir-, behandlet papir- og polymermembran – hverken under kort- eller langtidsstudierne.

Der var ingen indvirkning hverken af udetemperaturen eller af koncentrationen af sporgas på forholdet mellem overføringen af sporgas i papir- og polymermembranerne. Sporgasoverføringen gennem henholdsvis membranen af polymer og membranen af behandlet papir var 5 % og 13 %.

Content

Preface 6
Nomenclature 7
Introduction 8
Theoretical basics and literature review 8
Materials and Methods 17
Heat and enthalpy exchangers 17
Thermal and enthalpy performance test 18
Experimental setup 18
Experimental procedure 21
Gas transfer test 21
Experimental setup 21
Experimental procedure 22
Data analysis method 22
Uncertainties 24
Uncertainty in sensible effectiveness 24
Uncertainty in latent effectiveness 24
Leakage tests 26
Internal leakages 26
External Leakages 27
Results 28
Internal and external leakage 28
Short-term performance analyses 28
Influence of outdoor air temperature on effectiveness 28
Influence of face velocity on effectiveness 30
Long-term performance analyses 32
Performance of EX2 in terms of energy transfer rate. 34
Uncertainty 34
N_2O gas transfer 35
Influence of outdoor air temperature 35
Influence of N_2O concentration on transfer 36
Frost formation 38
Deformation in the membrane 38
Discussion 39
Performance in terms of thermal and enthalpy effectiveness 39
Performance in terms of gas transfer through the membrane 40
Performance analyses in terms of ice accretion 40
Deformation of the membrane 41
Advantages and disadvantages of membrane material 41
Advantages of using polymer membrane enthalpy exchanger 41
Disadvantages of using polymer membrane enthalpy exchanger 41
Conclusion 42
Phase 1. 42
Phase 2. 42
Phase 3. 42
Phase 4. 42
Appendix 44
Calibration/Co-calibration of HCS sensors 44
Calibration procedure 44
Bibliography 51

Preface

This report describes the outcomes of the research project “Performance analysis of membrane based air-to-air enthalpy recovery units” (Ydeevne af membranbaserede varme- og fugtgenvindere). The project has been carried out at the Danish Building Research Institute (SBi), Aalborg University Copenhagen. The project was financially supported by ELFORSK, a research and development program administrated by the Danish Energy Association under PSO project nr. 347-026. The project was completed under the supervision of Prof. Alireza Afshari and co-supervision of Senior researcher Niels Christian Bergsøe.

Danish Building Research Institute, Aalborg University Copenhagen
Department of Energy Performance, Indoor Environment and Sustainability of Buildings

Søren Aggerholm
Research Director

Nomenclature

S	Cross sectional area of channel	m^2
D	Diffusion coefficient of water vapour	$m^2/_s$
d_h	Hydraulic diameter	m
q_l	Latent heat transfer rate	W
l	Length of channel	m
h	Heat transfer coefficient	$W/_{m^2\,K}$
ṁ	Mass flow rate	$kg/_{sec}$
k_c	Mass transfer coefficient at channel wall surface	$kgm^{-2}s^{-1}Torr^{-1}$
N	Number of measurements	-
NTU	Number of transfer units	-
Nu	Nusselt number	-
u	Overall heat transfer coefficient	$W/_{m^2\,K}$
A_p	Partition plate area	m^2
p_w	Partial pressure of water vapour	$Torr$
K_{pa}	Permeability coefficient of water vapour in air	$kgm^{-1}s^{-1}Torr^{-1}$
RH	Relative humidity	%
A_f	Spacer plate area	m^2
q_s	Sensible heat transfer rate	W
SH	Sherwood numbers	-
h	Specific enthalpy of air	kJ/kg
h_{fg}	Specific enthalpy of water vapour	kJ/kg
C_p	Specific heat capacity of air	$J/_{kg.K}$
C_{vap}	Specific heat capacity of water vapour	$J/_{kg.K}$
C_{air}	Specific heat capacity of air	$J/_{kg.K}$
X	Specific humidity of air	$kg_{(water)}/kg_{(dry\ air)}$
T	Temperature	℃ or K
t	Time	s
U_T	Total uncertainty in temperature	-
U_ω	Total uncertainty in humidity ratio	-
U	Uncertainty	-
$U_{\varepsilon s}$	Uncertainty in sensible effectiveness	-
$U_{\varepsilon l}$	Uncertainty in latent effectiveness	-
R	Universal gas constant	$Torr\ m^3 kmol^{-1}K^{-1}$
z	Vertical axis	-
Q	Volumetric flow rate	$m^3/_s$

Greek letters

θ	Concentration of gas	ppm
ε	Effectiveness	-
$\emptyset$	Fin efficiency	-
η	Gas transfer ratio	-
ω	Humidity ratio	$kg_{(water)}/kg_{(dry\ air)}$
ε_l	Latent effectiveness	-
δ	Partition plate thickness	m
Φ	Relative humidity RH	%
σ	Standard deviation	-

Introduction

Use of heat recovery in mechanical ventilation systems is a requirement in the Danish building regulation. Conventionally, sensible heat is recovered, but due to high demands of appropriate indoor air quality with maximum possible energy saving, the focus on the total energy/enthalpy exchange is motivated. Air-to-air enthalpy exchangers have been in the market for several years. Generally, desiccant rotary wheel type enthalpy exchangers are used which are bulky, require maintenance and need power itself for rotation (Zhong et al., 2014). Recently, a new generation of enthalpy exchangers have been introduced, called membrane based enthalpy exchangers. The enthalpy exchangers are characterised as compact in size, stationary, and easy to construct (Kistler and Cussier, 2002; Zhang and Jiang, 1999). The technology itself is more than 30 years old but novel in terms of usage. Therefore, it is relevant to analyse the performance of enthalpy exchangers on long-term basis especially if to be used in cold climate such as in Scandinavia. The Danish Building Research Institute (SBi) at Aalborg University, Copenhagen has investigated the long-term and short-term performance of one heat and four enthalpy exchangers available in the market. The results will be useful for public authorities and building engineers to understand the performance of enthalpy exchangers and consequently the possibility of energy savings.

Theoretical basics and literature review

Energy recovery ventilation system is usually consists of energy recovery unit and mechanical ventilation system where a balanced airflow is provided between supply and exhaust in order to recuperate energy by tempering outdoor air with the indoor/stale air (Robbin et al., 2014). In heat recovery ventilation systems, sensible heat is recuperated whereas in energy recovery ventilation systems, both sensible and latent heat is recuperated. In enthalpy exchangers, the latent and total energy is recuperated due to the transfer of water molecules through the membrane. Molecular movement through membranes takes place in two steps. First water molecules transfer to the membrane surface by molecular diffusion. The second step is the transfer of molecules through the membrane, which may be through molecular diffusion, Knudsen diffusion, osmosis or a combination depending on the porosity of the membrane. Membranes are usually treated for the potential of diffusion through pores; therefore, the dominant mechanism is usually osmosis (Fisk et al., 1985).

Membrane based enthalpy exchangers were first introduced by Mitsubishi Japan in 1969 (Yoshino, 1969). Membrane based enthalpy exchangers differ from air-to-air sensible heat exchangers in the sense that the membrane-based medium can transfer heat as well as moisture without the size and complexity of the energy wheels (Yoshino, 1969).

In 1984, paper based enthalpy exchanger was analysed by (Tanaka, 1984). The paper was treated with hydrophilic resin and hygroscopic agents making the paper have selective porosity that allows transfer of the water molecule but not (or negligible) other gases. Tanaka (1984) used Eq. 1, 2, and 3 for sensible, latent and enthalpy transfer:

$$q_s = \dot{m} C_{air} \left(T_{f,0} - T_{f,i} \right) = \dot{m} C_{air} \left(T_{e,i} - T_{f,i} \right) \varepsilon_s \qquad Eq.1$$

Where q_s $[W]$ is the sensible heat transfer rate, $\dot{m}$ $[kg/s]$ is the mass flow rate, $C_{air}[J/kg/K]$ is the specific heat capacity of air, $T_{f,0}$ $[K]$ is the temperature of supply air coming out of the enthalpy exchanger, $T_{f,i}$ $[K]$ is the temperature of the outdoor air before entering into the enthalpy exchanger, $T_{e,i}$ $[K]$ is the tempearature of the extract air before entering into the enthalpy exchanger and ε_s is the sensible effectiveness of the enthalpy exchanger.

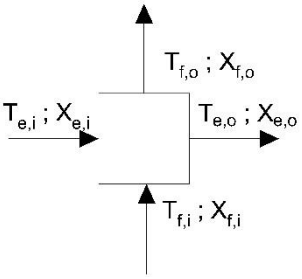

$$q_l = \dot{m}\{(h_{fg} + C_{vap}T_{f,o})X_{f,o} - (h_{fg} + C_{vap}T_{f,i})X_{f,i}\} \text{ or } \dot{m}\{(h_{fg} + C_{vap}T_{e,i})X_{e,i} - (h_{fg} + C_{vap}T_{f,i})X_{f,i}\}\varepsilon_l \qquad Eq.2$$

Where q_l $[W]$ is the latent heat transfer rate, h_{fg} $[kJ/kg]$ is the specific enthalpy of water vapour, $C_{vap}[J/kg/K]$ is the specific heat capacity of water vapour, $X_{f,o}$ $[kg_{water}/kg_{dry\ air}]$ is the specific humidity of supply air coming out of the enthalpy exchanger, $X_{f,i}$ $[kg_{water}/kg_{dry\ air}]$ is the specific humidity of the outdoor air before entering into the enthalpy exchanger, $X_{e,i}$ $[kg_{water}/kg_{dry\ air}]$ is the specific humidity of the extract air before entering into the enthalpy exchanger and ε_l is the latent effectiveness of the enthalpy exchanger. The enthalpy exchange can be estimated as:

$$q = q_l + q_s = \dot{m}(h_{f,o} - h_{f,i}) = \dot{m}(h_{e,i} - h_{f,i})\varepsilon \qquad Eq.3$$

Where q $[W]$ is the transfer of enthalpy, $h_{f,o}[kJ/kg]$ is the specific enthalpy of the supply air coming out of the enthalpy exchanger, $h_{f,i}[kJ/kg]$ is the specific enthalpy of the outdoor air before entering into the exchanger, $h_{e,i}[kJ/kg]$ is the specific enthalpy of the extract air before entering into the exchanger and ε is the total effectiveness of the enthalpy exchanger. Permeability coefficient was established by using Fick's law:

$$J = -\frac{Dm_v}{RT}\frac{dp_w}{dx} = -K_{pa}\frac{dp_w}{dx} \qquad Eq.4$$

Where D $[m^2/s]$ is the diffusion coefficient of water vapour in air under atmospheric pressure, m_v $[kg]$ is the mass of one mole of water vapour, R $[Torr\ m^3 kmol^{-1}K^{-1}]$ is the universal gas constant, p_w $[Torr]$ is the partial pressure of the water vapour, K_{pa} $[kgm^{-1}s^{-1}Torr^{-1}]$ is the permeability coefficient of the water vapour in the air.

K_{pa} is almost constant below 40 % RH and increase with further increase in humidity.

Airflow in the channels of the heat exchanger is laminar and the mass flow rate can be calculated as:

$$m_v = -\frac{4S}{d_h}\int_0^l K_{pa}\left(\frac{\partial p_w}{\partial r}\right)_{r=\frac{d_h}{2}} dz \cong m_v = k_c\frac{4S}{d_h}l\Delta P_{ln} \qquad Eq.5$$

Where S $[m^2]$ is the cross-sectional area of the channel, d_h $[m]$ is the hydraulic diameter, z is the vertical axis, l $[m]$ is the length of the channel, k_c $[kgm^{-2}s^{-1}Torr^{-1}]$ is the mass transfer coefficient at the channel wall surface, corresponding to the heat transfer coefficient h $[Wm^2K^{-1}]$.

Overall mass transfer coefficient K $[kgm^{-2}s^{-1}Torr^{-1}]$ corresponding to the overall heat transfer coefficient U $[Wm^{-2}K^{-1}]$ can be obtained from k_c and K_{pp} and is given by:

$$\mathrm{K} = \frac{1}{\mathrm{A_p}\left(\frac{1}{\mathrm{h_{m1}}(\mathrm{A_p} + \emptyset \mathrm{A_f})} + \frac{\delta}{\mathrm{K_{pp}A_p}} + \frac{1}{\mathrm{h_{m2}}(\mathrm{A_p} + \emptyset \mathrm{A_f})}\right)} \qquad Eq.6$$

Where $\mathrm{A_p}\ [m^2]$ is the partition plate area, $\mathrm{A_f}\ [m^2]$ is the spacer plate area $\emptyset$ is the fin efficiency, δ is the partition plate thickness, number 1 & 2 denote fluid 1 and fluid 2 respectively. Humidity effectiveness can be evaluated in a similar manner as of NTU method.

The capacity rate $\mathrm{C_m}[kgs^{-1}Torr^{-1}]$ of mass transfer corresponding to the capacity rate of heat transfer $\mathrm{C}[Js^{-1}K^{-1}]$ is given by:

$$\mathrm{C_m} = \frac{M_{vap}Q}{RT} \qquad Eq.7$$

Where $\mathrm{Q}\ [\mathrm{m}^3 s^{-1}]$ is the volumetric flow rate of the moist air.

$$\mathrm{NTU} = \frac{U_m A_p}{C_m} \qquad Eq.8$$

And humidity effectiveness is:

$$\varepsilon_\mathrm{l} = \frac{X_{1i} - X_{1e}}{X_{li} - X_{2i}} \qquad Eq.9$$

The exchanger's total water vapour transfer area on one side is:

$$\mathrm{A_t} = \mathrm{A_p} + \emptyset \mathrm{A_f} \qquad Eq.10$$

Tanaka (1984) used a total heat exchanger in the experiments and measured the dry bulb temperatures and wet bulb temperatures at two locations on each side of the exchanger. The author used several airflow rates to measure the effectiveness of the total heat exchanger. Moreover, Tanaka (1984) used Eq. 1 to 10 to predict the theoretical performances of the enthalpy exchanger.

Tanaka (1984) concluded that the mass transfer resistance is higher whereas thermal resistance of the paper is smaller than the expected one so the rate of heat transfer is dominated by air rather than by the paper. On the other hand, mass transfer rate is dominated by the paper.

A report on Ice formation issue over the surface of the residential heat exchanger was published by (Fisk et al., 1983). Ice formation may reduce the effectiveness of the heat exchanger down to 13.2 %. The decrease in effectiveness depends on the temperature and humidity of air streams and the duration of ice formation. For the surface temperature $\mathrm{T_{s,i}}$

$$\mathrm{T_{s,i}} = \frac{h_{w,i}T_{w,i} + h_{c,i}T_{c,i}}{h_{w,i} + h_{c,i}} \qquad Eq.11$$

Where $h_{w,i}\ and\ h_{c,i}$ are the convective heat transfer coefficient at location "i" and for the warm and cold airstreams, T is temperature, subscripts s, w, c, and i stands for the surface, warm, cold and point location respectively.

Condensation may effectively increase the warm air's convective coefficient due to a roughening effect of the surface and, thus, increase the heat transfer surface temperature. However, the coldest surfaces are generally located where the cold air enters the core and the convective coefficient for the cold air may be significantly increase in this region due to entrance effects. These two factors, condensation and entrance effects, counteract although one or the other may dominate in some situations. Ice formation may occur due to water vapour within the air if the dew point is below 0 °C or if the air below the surface is cooled below its dew point. As ice or frost forms in the core of the heat exchanger, the temperature efficiency decreases. The average rate of change of efficiency for a freeze cycle, $\Delta\varepsilon$, which is a measure of the rate of performance deterioration, was calculated from the Eq.12.

$$\Delta\varepsilon = \frac{\varepsilon_3 - \varepsilon_n}{t_n - t_3} \qquad Eq.12$$

Where ε_3 is the value of effectiveness calculated from the data recorded during the third five-minute data interval after completion of the previous defrost, ε_n is calculated from data taken in the last interval prior to initiating the next defrost, and t is the corresponding times. The onset of freezing as determined by visual observation ranged between -3 °C and -12 °C and was a function of both heat exchanger design and humidity of the airstream.

(Kim, 1985) evaluated performance of heat exchanger in terms of thermal effectiveness factor (enthalpy effectiveness E) and temperature recovery factor (sensible effectiveness TR). It is experimentally found that E and TR are independent of outdoor temperature and 58 % and 72 %, respectively. Some data points deviated from the rest due to reduced exhaust airflow, which in turn was due to frost build-up on the heat exchanger core.

A detailed heat and mass transfer model for energy recovery ventilation with a porous hydrophilic membrane core was presented by (Zhang and Jiang, 1999). It is found that in the cross-flow arrangement, the membrane cannot be used effectively to exchange enthalpy.

(Niu and Zhang, 2001) studied the enthalpy transfer in cross-flow exchanger with hydrophilic membrane core. The simulated and experimental results are compared in this study. The variations in sensible and latent effectiveness is calculated with various operating conditions and materials. The sensible effectiveness is determined by the NTU-method (Number of Transfer Units) whereas latent effectiveness is influenced by both the material and the operating conditions like outdoor air temperature, relative humidity and airflow. The thermal diffusive resistance is constant and moisture diffusive resistance is not. The moisture resistance is determined by the slopes of sorption curves and the operating conditions. A new dimensionless parameter is introduced which reflects the effects of operating conditions on the mass diffusive resistance. This parameter is defined as the coefficient of mass diffusive resistance (CMDR). By comparing the performances with different membrane materials, it is revealed that the membrane material with a linear sorption curve performs better than other materials under common.

(Zhang et al., 2008) studied three types of enthalpy exchangers. Three exchangers are based on paper, CA (Cellulose Acetate) membrane and CA modified membrane. The authors investigated the influence of outdoor air conditions on sensible and latent effectiveness. Sorption curves and contact angles of these three materials are measured to reflect their hydrophilicity. The steady-state sensible and latent effectiveness of the three exchangers are studied in a test rig, and the test results are compared with the model predictions. A heat and moisture transfer model for the enthalpy exchangers is proposed. The effects of the varying operating conditions like airflow rates, temperature, and humidity on the sensible and latent effectiveness are evaluated. Both the numerical and experimental results indicate that the moisture resistance through plates is co-determined by thickness, sorption slope, and sorption potential. Moisture diffusivity in various materials is in the same order. When the membrane thickness is fixed, the higher the sorption slopes are, the higher the latent performance is. Of the three exchangers, the exchanger with the modified CA membrane material has the highest performance due to small thickness, steep sorption slope, and large sorption potentials. The paper exchanger has a latent effectiveness of 0.4, while the membranes have latent effectiveness of greater than 0.7.

In Figure 1, Figure 2, and Figure 3, Mem 1 and Mem 2 stands for cellulose acetate and modified cellulose acetate membranes respectively.

As shown in Figure 1 and Figure 2 contrary to sensible effectiveness, the latent effectiveness is quite different for three exchangers. The paper exchanger has the lowest latent effectiveness. The modified CA membrane exchanger has the highest effectiveness. The CA membrane and modified CA membrane exchangers have latent effectiveness 60 % higher than the paper exchanger does. The reason lies in several factors: (1) The membranes thickness are 10 % of the thickness of the paper; (2) The moisture diffusivities in membrane are 70 % higher than in paper; (3) Maximum moisture uptake in modified cellulose acetate membrane is 1.7 times higher than in paper. All these factors contribute to the fact that modified cellulose acetate membrane has latent effectiveness of 0.7, while the paper exchanger has a latent effectiveness of 0.4. The reason why different plate materials have such different results is that the plate accounts for a large portion of the total moisture resistance.

Figure 3 shows the variations of latent effectiveness with varying outdoor air temperature for the three exchangers. As seen, generally, the higher the outdoor air temperature, the higher the latent effectiveness. The trends are the same for the three exchangers.

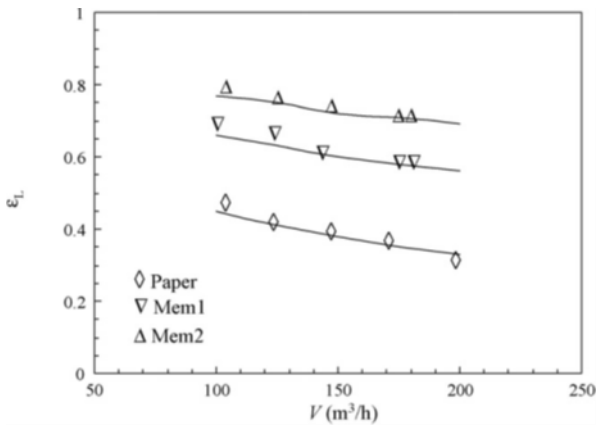

Figure 1 Variation in latent effectiveness with outdoor airflow rate (Zhang et al., 2008)

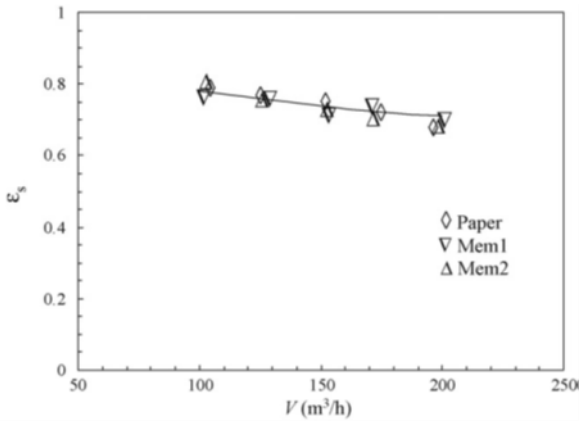

Figure 2 Variation in sensible effectiveness with outdoor airflow rate (Zhang et al., 2008)

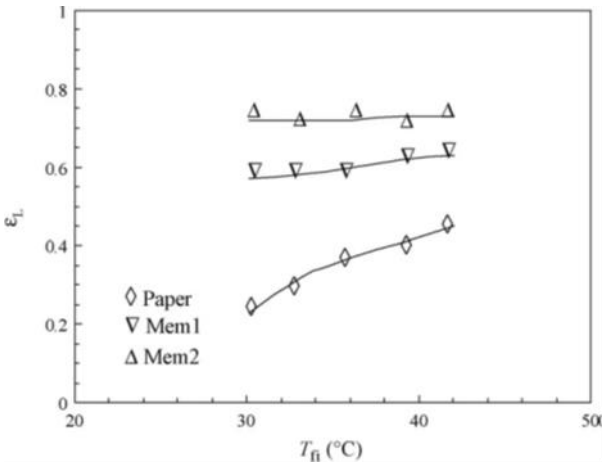

Figure 3 Variation in latent effectiveness with outdoor air temperature (Zhang et al. 2008)

From these experiments, Zhang et al., (2008) concluded that due to the negligible sensible heat resistance, all three exchangers have the same high sensible effectiveness. The authors also concluded that (1) Material properties and operating conditions have little influences on exchanger's sensible heat performance. (2) Moisture transfer resistance through plates is substantial. Therefore, both the material properties and operating conditions have impacts on latent effectiveness. Of the influencing factors, plate thickness is a determining factor. The thinner the transferring medium is, the less the resistance is. The modified CA membrane has a very high latent effectiveness. It is also insensitive to outside operating conditions.

(Liu et al., 2014) investigated the ice formation limits in membrane based energy exchanger (MEE). A model to calculate frosting limits for pure counter-flow MEE is developed through combining condensation limits and critical outdoor air temperature. The model is employed to calculate the frosting limits in Oslo, Norway climate with designated membrane. The author concluded that,

- Acceptable maximum indoor relative humidity is approximately 30 % to ensure frost-free operation for MEE with the sensible effectiveness being 0.7 when the lowest outdoor air temperature is -20 °C.
- When the outdoor air temperature is higher than -8 °C, frost will not happen at any indoor moisture level for MEE with sensible effectiveness being 0.7.
- The higher sensible effectiveness recommended by the existing standard will lead to a higher frosting risk. It probably results in consuming more energy to defrost. The combination of sensible and latent effectiveness is superior to ensure frost-free operation for MEE.

(Zhong et al., 2014) investigated the energy exchange on different membranes and structures. The authors used three different types of membranes and three different structures. The purpose of this study was to find the most suitable membrane material and structure of energy recovery. The structures used in this study are parallel-plate, plate-fin and cross-corrugated. The membranes used for this work are; one-step hand-made cellulose acetate membrane, hydrophobic-hydrophilic composite membrane, and machine-made cellulose acetate membrane. The study shows that the airflow rates have an influence on the sensible and latent effectiveness. The effect of inlet humidity is negligible for sensible effectiveness. However, it has an impact on latent effectiveness. Higher the inlet humidity, the larger the latent effectiveness is reported. Secondly, cross-corrugated plate is suggested for the best energy recovery. Thirdly, the hand-made cellulose acetate membrane is suggested for the total heat recovery. These suggestions are made based

on the relation between 1) effectiveness and relative humidity; 2) effectiveness and Nusselt and Sherwood numbers and 3) effectiveness and airflow rates.

From Figure 4 and Figure 5, Zhong et al., (2014) concluded that the airflow rates have an impact on cores sensible and latent effectiveness. Both sensible effectiveness and latent effectiveness decline with the increased airflow rates.

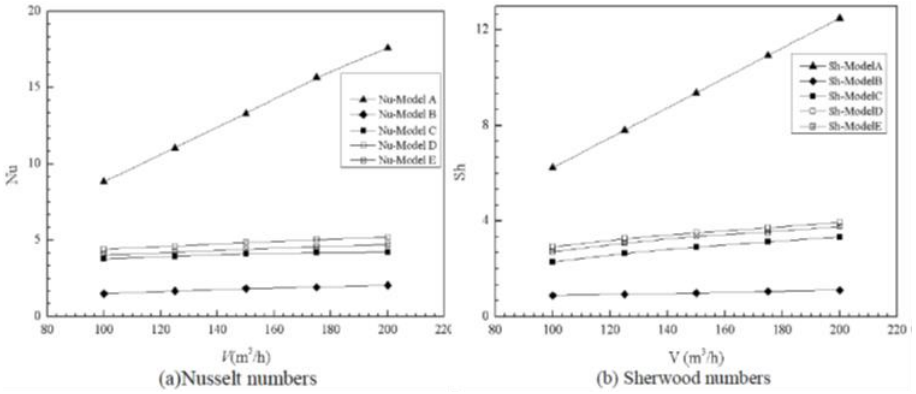

Figure 4 Nusselt and Sherwood numbers with varying air flow rates (outdoor air inlet 35 °C and 70 %RH, exhaust air inlet 27 °C and 50 %RH) (Zhong et al., 2014)

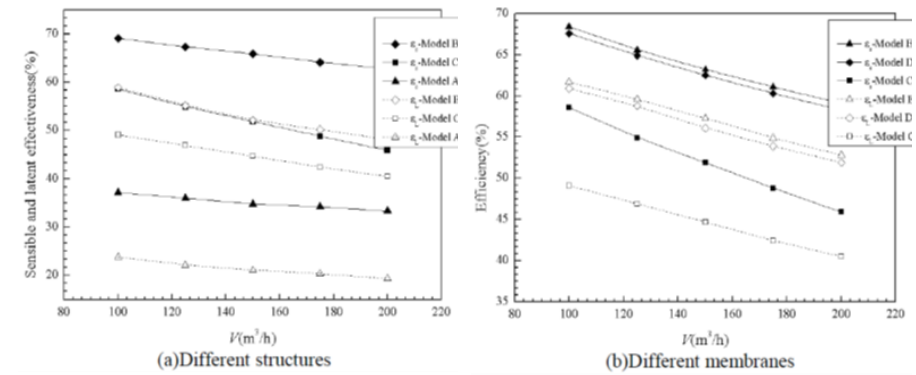

Figure 5 Variations of sensible and latent effectiveness with air flow rates (outdoor air inlet 35 °C and 70 %, exhaust air inlet 27 °C and 50 %) (Zhong et al., 2014)

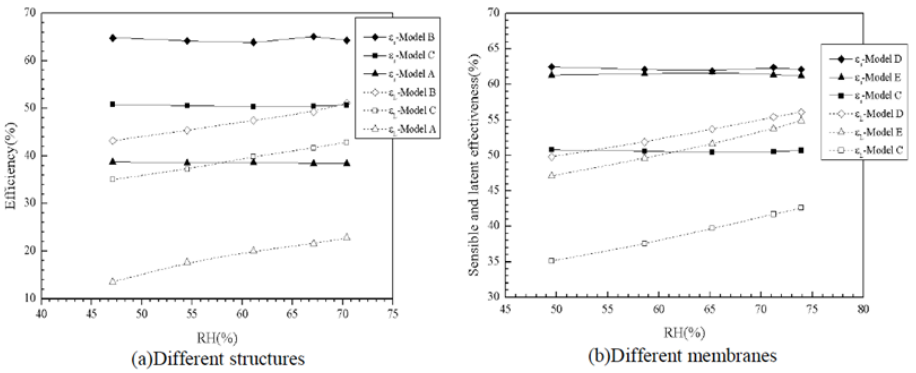

Figure 6 Variations of sensible and latent effectiveness with inlet relative humidity (both inlet air rates are 150 m/h, outdoor air inlet 35 °C and exhaust air inlet 27 °C and 50 %RH) (Zhong et al., 2014)

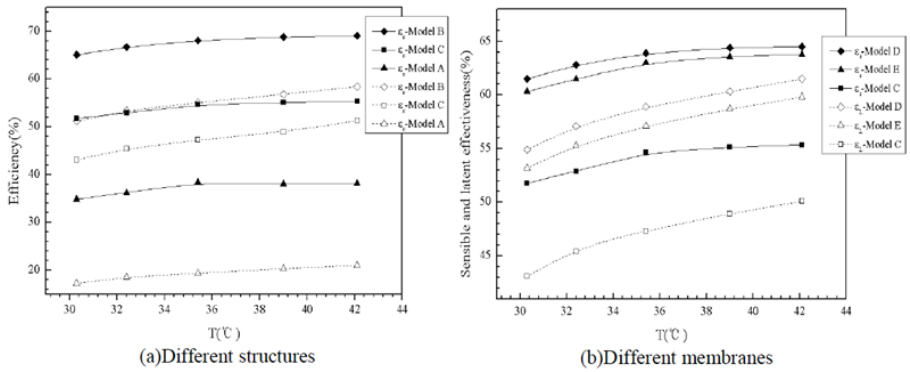

Figure 7 Variations of sensible and latent effectiveness with inlet air temperatures (both inlet air rates are 150 m³/h, outdoor air inlet 35 °C, exhaust air inlet 27 °C and 50 %RH) (Zhong et al., 2014)

From Figure 6 and Figure 7, it is concluded that the effect of inlet humidity on sensible effectiveness can be neglected, but for latent effectiveness, the higher the inlet humidity is, the larger the latent effectiveness will be. Under the varied temperature conditions, the sensible effectiveness is less sensitive to temperature variation than latent effectiveness.

(Nasr et al., 2015) studied ice formation and its effect on energy consumption in heat exchangers. They proposed two methods and their comparison to minimize the energy consumption. In this study, the performance of two cross-flow heat/energy exchangers at frosting and defrosting periods are analysed under different operating conditions and the values of frosting limit and defrosting time ratio are presented. As well, the effects of these two defrosting methods on energy consumption of ventilation in three cold cities (i.e. Saskatoon, Anchorage and Chicago) were evaluated. Nasr (2015) concluded that frosting commonly occurs inside heat/energy exchangers in cold climates. It is found that the values of defrosting time ratio (DTR) of heat/energy exchangers increases as the outdoor air temperature decreases. Correspondingly, the average effectiveness values of the heat/energy exchangers in the complete operating period decrease as the outdoor air temperature decreases. In addition, the average sensible effectiveness of the heat exchanger is much lower than the average effectiveness of energy exchanger. The influences of two defrosting methods for air-to-air heat/ energy exchangers, outdoor air preheating and outdoor airflow bypassing methods, on energy consumption of ventilation are evaluated in three cold cities. The results show that the outdoor air preheating method performs much better than the outdoor air bypassing method, especially for the heat recovery exchanger. The saving percentage using preheating method is 44 %, which is twice of the saving using the bypassing method (22 %) for the heat exchanger in Saskatoon. Based on this finding, the frosting limit detection of heat/energy exchangers is important and more research is needed in future work. The results also show that the heat/energy saving potential in Saskatoon has the largest reduction under frosting conditions, while there is the smallest reduction in Chicago. The reason is that Saskatoon is the coldest among the three cities and the freezing period is the longest. The outdoor weather conditions have influence on the frosting in exchangers and energy consumption for ventilation.

(Andersson et al., 1993) investigated the mass transfer of contaminants in rotary enthalpy exchangers. They studied re-entrainment of a tracer gas formaldehyde via six rotary air-to-air heat exchangers (all enthalpy exchangers) in the northern part of Sweden. Five exchangers were installed in office buildings and one in a day-care centre. Formaldehyde in indoor is used as a monitor pollutant and is determined in air samples collected in the ducts at four positions around the rotor of the exchanger, in the supply-air duct and in the exhaust-air duct. The sample analysis of formaldehyde is made by high-

performance liquid chromatography. The re-entrainment of formaldehyde is calculated and found to be 1-9 %.

(Nie et al., 2015) investigated the re-entrainment of the gases through the polymer membrane. They used three different gases to evaluate the mass transfer through the polymer membrane. Experimental studies are conducted in a laboratory setting to investigate the enthalpy efficiency and gas-phase contaminant transfer in a polymer membrane enthalpy recovery unit. One polymer membrane enthalpy recovery unit is used as a reference unit. Simulated indoor air and outdoor air by twin chambers are connected to the unit. Three chemical gases are dosed to the indoor exhaust air to mimic indoor air contaminants. Based on the measurements of temperature, humidity ratio, and contaminant concentrations of the indoor exhaust air and outdoor air supply upstream and downstream of the unit, the temperature efficiencies, humidity efficiencies, enthalpy efficiencies, and contaminant transfer ratios are calculated. The results show that over 60 % of enthalpy recovery efficiency can be achieved and that the contaminant transfer ratios are in the range of 5.4 % to 9.0 %. The enthalpy efficiency in cold–dry climate conditions is slightly higher than in hot–humid climate conditions. The contaminant transfer ratio is independent of any hygrothermal difference between indoor and outdoor air and is unrelated to its molecule size or water solubility.

Nie et al., (2015) used Eq. 13 to calculate the contaminant transfer through the membrane.

$$\eta_m = \frac{m_{supply} - m_{outdoor}}{m_{indoor} - m_{outdoor}} \qquad Eq.13$$

Where η_m is the gas-phase contaminant transfer ratios, m_{supply}, $m_{outdoor}$, m_{indoor} are the concentrations of the monitored contaminant in the supply air, outdoor air, and indoor air [mg/m^3] respectively.

Many scholars and researchers have analysed the performance of heat and enthalpy exchangers. The studies focused on short-term experimental analysis. There was is deficiency of knowledge of performance of enthalpy exchanger in long-term operation under cold climate. The focus of current work was to analyse the performance of enthalpy exchangers for long-term along with short term under different operating conditions. The ice accretion on the enthalpy exchangers and gas transfer through the membrane is also studied.

Materials and Methods

The work was divided into four phases in order to evaluate (1) thermal and enthalpy performance of heat and enthalpy exchanger (2) N_2O gas transfer ratio through membrane of enthalpy exchanger (3) ice formation on the fins of enthalpy exchanger (4) deformation in the membrane of the enthalpy exchanger.

In the first phase, one heat exchanger (HX1) and four different enthalpy exchangers (EX1, EX2, EX3 and EX4) were studied for short term thermal and enthalpy performance. Afterwards EX2 was selected for the long-term performance test under different operating conditions.

In the second phase, the N_2O gas transfer ratio in the membrane of enthalpy exchanger was studied. One polymer membrane based and one treated paper membrane based enthalpy exchangers were selected for this study. The selection of the enthalpy exchangers were based on short-term performance tests. The transfer ratio was studied at different conditions i.e. at different outdoor air temperatures and at different gas concentrations.

In the third phase, the ice formation in the membrane based enthalpy exchanger was studied under different operating conditions.

In the fourth phase, deformation of the membranes of enthalpy exchangers was studied.

Heat and enthalpy exchangers

In this study, one sensible heat exchanger and four enthalpy exchangers of different sizes, flow arrangements, and membrane structures were analysed in terms of energy saving. The physical properties and structures of the sensible and enthalpy exchangers are shown in Table 1.

Table 1 Physical properties of heat and enthalpy exchangers

Type	Membrane Material	Dimension mm^3	Flow type	Membrane Structure
HX1 Sensible heat exch.	Polymer 1 (Plastic)	366x366x500	Quasi Counter	Parallel plate
EX1 Enthalpy exchanger	Polymer 2	366x366x500	Quasi Counter	Parallel plate
EX2 Enthalpy exchanger	Polymer 3	366x366x500	Quasi Counter	Parallel plate
EX3 Enthalpy exchanger	Paper	200x200x500	Cross	Plate-fin
EX4 Enthalpy exchanger	Treated paper	200x200x300	Cross	Plate-fin

Figure 8 (a) shows the quasi-counter flow arrangement in heat/enthalpy exchanger and Figure 8 (b) shows the cross flow arrangement of enthalpy exchanger. Figure 9 shows the parallel plate channels and Figure 10 shows the plate-fin channels. Each channel in parallel plate type is rectangular and each channel in plate-fin type is triangular.

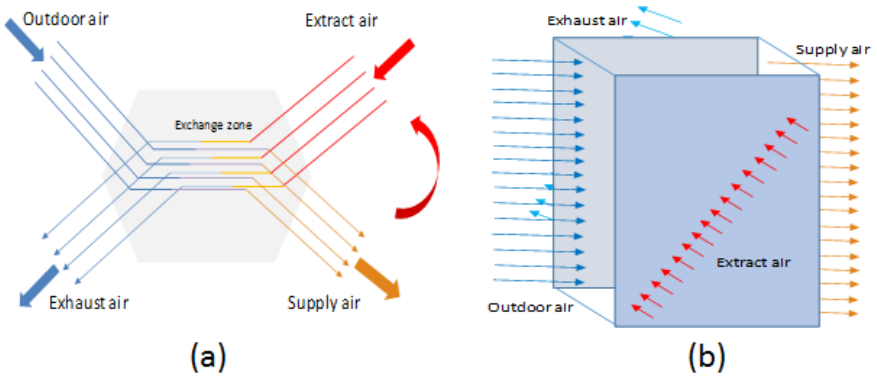

Figure 8 (a) Quasi counter flow (b) Cross flow.

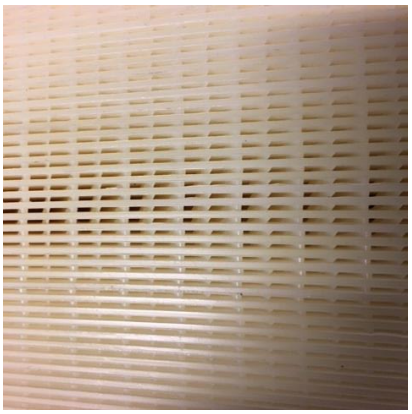

Figure 9 Parallel plate exchanger

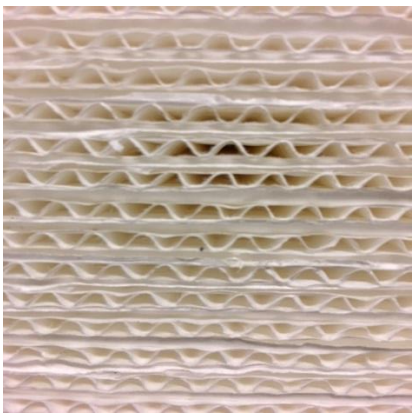

Figure 10 Plate-fin exchanger

Thermal and enthalpy performance test

The first phase was to calculate the thermal and enthalpy performance of one heat and four enthalpy exchangers under different operating conditions.

Experimental setup

A test rig was built in the laboratory at SBi (Statens Byggeforskningsinstitut) to analyse the thermal and enthalpy performance of air-to-air heat and enthalpy exchangers. In the test rig, it was possible to analyse air-to-air parallel plate heat/enthalpy exchangers of different geometries at different operating conditions (outdoor air temperature, relative humidity and airflow). The minimum outdoor air temperature values used in this study were according to Danish reference year.
The test rig consist of the following four sections:

1. Cooling machine

Cooling machine was equipped with a fan and a refrigeration system. The air temperature and speed of the fan could be set manually. Defrosting cycle in the cooling machine could be set according to the requirement. The cooling machine had the ability to deliver cold air below -20 °C. Cooling machine is shown in Figure 13.

2. Chamber 1

The chamber 1 was a box made up of plywood. The box was thermally insulated from inside and outside. The box was painted from inside which kept it airtight. At the inlet and outlet (air) of the test chamber, humidity and temperature sensors were installed in order to measure the temperature and relative humidity. A humidifier was installed inside of the chamber 1 with the continuous water level controlling system (mechanical system). To control

the humidity levels in the chamber 1, a humidity sensor with 220 V output signal was provided. Chamber 1 is shown in Figure 12.

3. Test chamber

The test chamber consist of four compartments and in the middle of the chamber the heat/enthalpy exchanger to be analysed was inserted. On each side of heat/enthalpy exchanger, five surface temperature sensors were attached to analyse heat transfer characteristics of heat/enthalpy exchangers.

Moreover, on each side of the exchanger, three temperature and humidity sensors were mounted at 1 cm distance from the face of heat/enthalpy exchanger to analyse the effectiveness of the exchanger. Moreover, one temperature and humidity sensor was installed at the inlets/outlets of the test chamber.

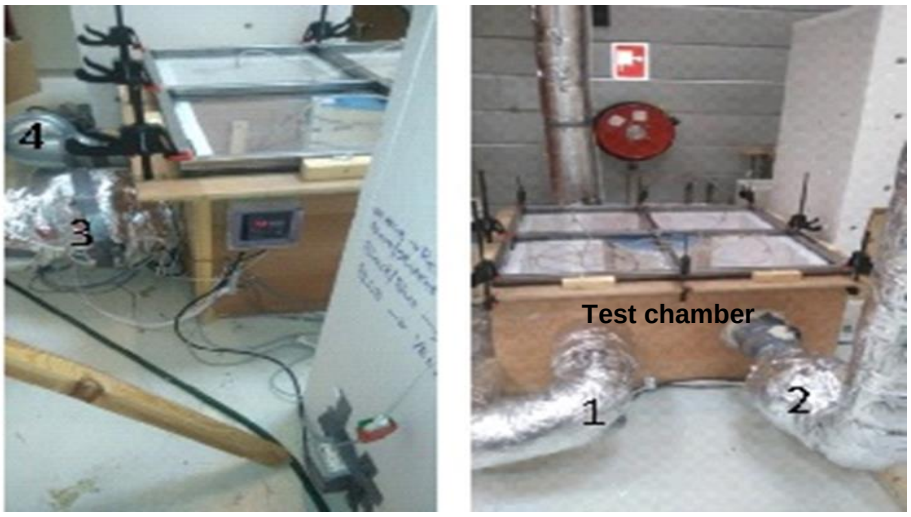

Figure 11 Airflow arrangement. outdoor air (1), indoor air (2), exhaust air (3) and supply air (4).

The test chamber was thermally insulated except the top part, which was transparent plastic for visualization. See Figure 11. Likewise, on each side of the test chamber, a pressure tap was provided to measure the pressure drop. On indoor airside and supply airside, constant speed fans were installed and on exhaust airside, a variable speed fan was installed as shown Figure 14. These fans were included in the flow circuit to increase the flow rates. However, the fans were not selected based on calculations. Therefore, there is a possibility that the pressure drops and flows on each side of the exchanger would not be typical. However, when all the fans are turned off except the cooling machine fan, the pressure drop and the effectiveness on each side of the exchanger should be same.

The flow meters on the outdoor airside and indoor airside were installed to characterize the effectiveness. Pressure difference was measured manually by a digital handheld manometer (EMA 150 from Halstrup Walcher) in order to calculate the flow rate.

4. Chamber 2

Chamber 2 was of same geometrical dimensions as of chamber 1, see Figure 12. In chamber 2, a humidifier was installed. The relative humidity setpoint was 60 %, which resulted in 50 % relative humidity in the chamber 2. A continuous water supply system was attached to the humidifier. Radiators were provided inside the chamber 2 to control the temperature. The radiators were set at 21 °C.

Figure 12 Chamber 1 and chambers 2

Figure 13 Cooling machine and the duct work

Data acquisition system and sensors

Campbell data acquisition system

The data acquisition system (CAMPBELL data logger CX-1000) was used to retrieve the data from different sensors. The data acquisition system was mounted on the wall next to the test rig in two boxes which were connected to each other, power and to the computer. To log the measured data, several sensors were installed in the system. Two type of sensors (Temperature probe 107 and 110PV-L) were attached to the surfaces of the heat exchanger to examine the heat transfer properties. The details of theses sensors are given below:

Temperature sensors for surface temperature

The temperature sensors type 107 is a rugged, accurate probe that measures the temperature of the air from -35 °C to +50 °C with an inaccuracy limit of ± 0.1 ºC.

Surface temperature sensors

Another type of temperature sensor 110PV-L by CAMPBELL SCIENTIFIC range from (-40 °C to +135 °C with an inaccuracy limit of ± 0.2 ºC) was used to measure the surface temperature by direct contact. It typically monitors the temperature of a photovoltaic module, but can also monitor the temperature of other devices. This thermistor was compatible with the data logger and is ideal for solar energy applications. Four of 110PV-L type sensors were stuck to measure the temperature on the heat/enthalpy exchanger surface with the interval of 1 minute.

Temperature and humidity sensors

The HCS i.e. first generation, manufactured by Rotronic, (range from -40 °C to 85 ºC and 0 to 100 % relative humidity with an inaccuracy limit of ± 0.1 ºC and 2%RH) was a rugged temperature and humidity probe that was used to measure the temperature and humidity for short and long term experiment with the measuring interval of 1 minute. The probe included a filter to protect the sensor from dust and particles. All the HCS sensors were calibrated/co-calibrated before starting measurements. The detailed report regarding the calibration of sensors is shown in the Appendix.

Barometric pressure sensor

The CS106, manufactured by Vaisala, measures barometric pressure for the range of 500 to 1100 mbar with an inaccuracy limit of ± 0.3 mbar. The barometric pressure was required to convert relative humidity to absolute humidity.

Experimental procedure

The flow diagram of experimental procedure is shown in Figure 14. The numbers 1, 2, and 3 show the number of fans and the alphabets A, B, C, and D show the four sections of the test setup. Air temperature was regulated to a desired temperature in the cooling machine. The cooled air passed through chamber 1 where (if required) humidity could be increased. Air from the chamber 1 then entered into the test chamber where it passed through a heat exchanger. Air from the test rig (supply airside of the heat exchanger) then delivered into the chamber 2 through a fan (Fan 2). In chamber 2, the air was conditioned to the room temperature by using a heating device and a humidifier. The air from chamber 2 then delivered into the test rig using a fan (Fan 1). This indoor air passed through the extract side of the heat exchanger. Hence, heat/enthalpy exchanged between outdoor air stream and the indoor air stream. Finally, air from the heat exchanger exhausted and delivered back to the cooling machine through a fan (Fan 3).

All the air ducts were insulated. Two air filters were installed in the ducts of outdoor and indoor air.

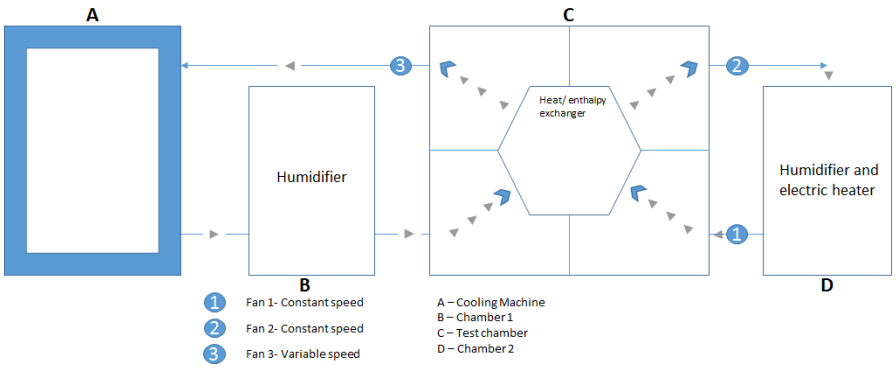

Figure 14 Flow diagram of the thermal and enthalpy performance analyses test setup

Gas transfer test

Experimental setup

The experimental setup for testing the transfer of gas through the membrane of enthalpy exchangers was consist of the Nitrous oxide (laughing gas) and multi-gas monitor.

Nitrous oxide (N_2O)

N_2O was used as a tracer gas. N_2O gas is colourless and non-flammable at room temperature. The molar mass of N_2O gas is 44.013 g/mol, which is greater than the molar mass of water (H_2O) which is 18.015 g/mol. The solubility of N_2O gas in water is 1.5 g/L at 15 °C. The concentration of N_2O in outdoor air is about 328 ppb.

Multi-gas monitor

Multi-gas monitor type 1302 by Brüel and Kjær was used to measure the gas concentration. The multi-gas monitor is a micro-processor-controlled monitor, which has the ability to measure five different gases and water vapour in any gas mixture. The lowest detection limit of N_2O gas is 0.5 ppm and the highest detection limit is 100,000 times the lowest detection limit. Measurement of five gases and water vapour takes 105 seconds.

Experimental procedure

Schematic of tracer gas contaminant transfer through the membrane is shown in Figure 15.

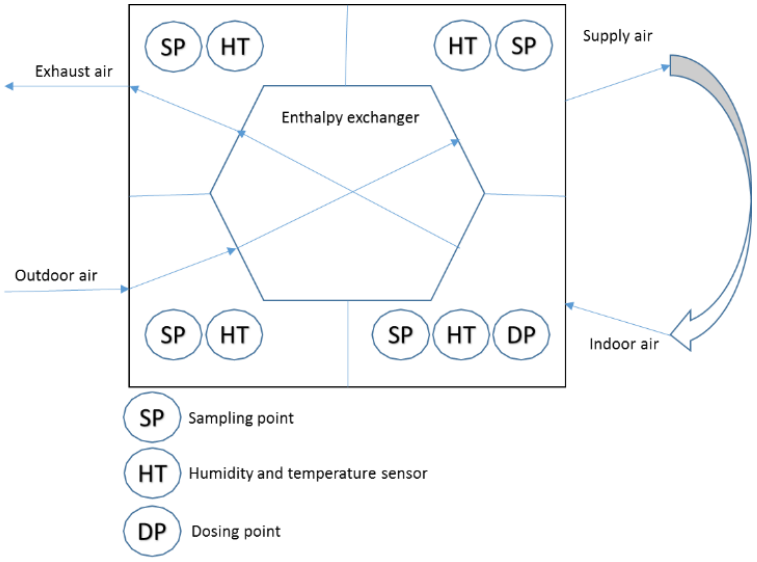

Figure 15 Flow diagram of tracer gas (N_2O), transfer test setup

Continuous flow of tracer gas (N_2O) was supplied at dosing point (DP) until it reached the steady state. When the concentration of the gas was constant at indoor airside, the concentration was measured at all the sampling points (SP) around the enthalpy exchanger. The humidity and temperature sensors (HT) were mounted on all sides of the enthalpy exchanger in order to measure the relative humidity and temperature.

Data analysis method

A heat and mass transfer model, Eq. 14, was used to calculate the effectiveness ANSI/ASHRAE standard 84 (2013). Eqs. 15, 16 and 17 are derived from Eq. 14.

Operating conditions (outdoor temperature, humidity ratio, and mass flow rate) have an impact on the performance of enthalpy exchangers. The performance of enthalpy exchanger is determined by its effectiveness. Eqs. 15, 16 and 17 were used to calculate the sensible, latent and the total effectiveness respectively.

$$\varepsilon = \frac{C\left(X_{supply\ air} - X_{outdoor\ air}\right)}{C_{min}(X_{indoor\ air} - X_{outdoor\ air})} \qquad Eq.14$$

In Eq. 14, C is the capacity rate and C_{min} is the minimum capacity rate between supply and exhaust air. It can be denoted as:

$C = \dot{m}C_p$ for sensible effectiveness where $\dot{m}$ is the mass flow rate in $\left[{}^{kg}/_{sec}\right]$ and C_p is the specific heat capacity of air in $\left[{}^{J}/_{kg.℃}\right]$.

$C = \dot{m}h_g$ for latent effectiveness where $\dot{m}$ is the mass flow rate in $\left[{}^{kg}/_{sec}\right]$ and h_g is the enthalpy of dry saturated water vapours in $\left[{}^{kJ}/_{kg}\right]$.

$C = \dot{m}$ for total effectiveness where $\dot{m}$ is the mass flow rate in $\left[{}^{kg}/_{sec}\right]$

X can be replaced with T, ω, and h while calculating sensible, latent and total effectiveness. In this study, closed air loop system is used and the airflow rates are equal on supply and exhaust side. Subsequently, the Eq. 14 can be expressed as:

$$\varepsilon_s = \frac{\left(T_{supply\ air} - T_{outdoor\ air}\right)}{\left(T_{indoor\ air} - T_{outdoor\ air}\right)} \qquad Eq.15$$

$$\varepsilon_l = \frac{\left(\omega_{supply\ air} - \omega_{outdoor\ air}\right)}{\left(\omega_{indoor\ air} - \omega_{outdoor\ air}\right)} \qquad Eq.16$$

$$\varepsilon_t = \frac{\left(h_{supply\ air} - h_{outdoor\ air}\right)}{\left(h_{indoor\ air} - h_{outdoor\ air}\right)} \qquad Eq.17$$

In Eqs. 15, 16 and 17 ε_s , ε_l, ε_t is the sensible energy effectiveness, latent energy effectiveness, and total energy effectiveness, T [℃] is the temperature, ω $\left[kg_{water}/kg_{dry\ air}\right]$ is the humidity ratio and h $\left[{}^{kJ}/_{kg}\right]$ is the total enthalpy. The total enthalpy can be calculated as:

$$h = T + \omega h_g \qquad Eq.18$$

Where T is dry bulb temperature in [℃] and ω is humidity ratio in $\left[kg_{water}/kg_{dry\ air}\right]$

$$h_g = 2501 + 1.86T \qquad Eq.19$$

The expressions for maximum possible sensible, latent and the total energy recovery and the actual sensible, latent and the total energy recovered is shown in Eqs. 20, 21 and 22.

$$q_{\max(s)} = \dot{m}C_p(T_{indoor\ air} - T_{outdoor\ air})$$
$$q_s = \varepsilon_s q_{\max(s)} \qquad Eq.20$$

$$q_{\max(l)} = \dot{m}h_{fg}(\omega_{indoor\ air} - \omega_{outdoor\ air})$$
$$q_l = \varepsilon_l q_{\max(l)} \qquad Eq.21$$

$$q_{\max(t)} = \dot{m}(h_{indoor\ air} - h_{outdoor\ air})$$
$$q_t = \varepsilon_t q_{\max(t)} \qquad Eq.22$$

Where $q_{\max(s,l,t)}$ $[kW]$ is maximum possible sensible, latent, and total energy transfer rates, and $q_{s,l,t}$ $[kW]$ is the actual sensible, latent, and total energy transfer rates.

To calculate the gas transfer ratio through polymer membrane and treated paper membrane, Eq. 23 was used.

$$\eta_\theta = \frac{\left(\theta_{supply\ air} - \theta_{outdoor\ air}\right)}{\left(\theta_{indoor\ air} - \theta_{outdoor\ air}\right)} \qquad Eq.23$$

Where η_θ is the gas transfer ratios; $\theta_{supply\ air}, \theta_{outdoor\ air}$, and $\theta_{indoor\ air}$ are measured concentrations of monitored gas in the supply air, outdoor air and indoor air $[ppm]$ respectively.

Uncertainties

Here two types of errors are considered. 1. Systematic/bias errors (U_s), 2. Random errors (U_r). Systematic errors results from calibration errors or instrumental drift. Random errors are caused by the changes in the experimental environment.
To calculate the uncertainty in the measured quantities, the following equations were used.

$$\Delta x = \sigma = \sqrt{\frac{\sum_{i=1}^{N}(x_i - x_{avg})}{N}} \qquad Eq.24$$

Where: $x_{avg} = \frac{\sum_{i=1}^{N} x_i}{N}$ is the mean value of the measured quantity, N is the number of measurements and σ is the standard deviation of the measured quantity. The majority of data lies in the range: $x_{avg} \pm \sigma$
The random uncertainty of the mean value was calculated from the following formula:

$$U_r = \frac{\Delta x}{\sqrt{N}} \qquad Eq.25$$

Total uncertainty U in a set of measured quantity can be calculated as:

$$U = \sqrt{U_r^2 + U_s^2} \qquad Eq.26$$

In Eq. 26, U_r is random uncertainty and U_s is the systematic uncertainty.
From Eq. 26, following expressions can be drawn.

$U_T = \sqrt{U_r^2 + U_s^2}$

Where U_T is the total uncertainty in the measured temperature.

Uncertainty in sensible effectiveness

To calculate the uncertainty in sensible effectiveness, Eq. 27 was used:

$$U_{\varepsilon s} = \sqrt{\begin{aligned} &\left(\frac{1}{T_{outoor\ air} - T_{indoor\ air}}\right)^2 U^2_{T\ Supply\ air} \\ &+\left(\frac{T_{supply\ air} - T_{indoor\ air}}{(T_{outoor\ air} - T_{indoor\ air})^2}\right)^2 U^2_{T\ outdoor\ air} \\ &+\left(\frac{T_{outdoor\ air} - T_{supply\ air}}{(T_{outoor\ air} - T_{indoor\ air})^2}\right)^2 U^2_{T\ indoor\ air} \end{aligned}} \qquad Eq.27$$

Where: $U_{\varepsilon s}$ is the total uncertainty in sensible effectiveness,
$U_{T\ supply\ air}, U_{T\ outdoor\ air}\ and,\ U_{T\ indoor\ air}$ is the total uncertainty in the temperature of the supply air, outdoor air and the indoor air,
$T_{outdoor\ air},\ T_{indoor\ air},\ and\ T_{supply\ air}$ is the temperature of outdoor air, indoor air and supply air in [℃] respectively (Farrington and Wells, 1986).

Uncertainty in latent effectiveness

To calculate the total uncertainty in the measured humidity ratio, following expressions were used.

$$\omega = \frac{\Phi * 10^7}{6.19 * e^{5427/T}}$$

$$U_\omega = \pm\sqrt{(\frac{\partial\omega}{\partial\Phi}U_\Phi)^2 + (\frac{\partial\omega}{\partial\mathrm{T}}U_\mathrm{T})^2}$$

$$U_\omega = \pm\sqrt{(\frac{10^7}{6.19 * e^{5427/T}}U_\Phi)^2 + (\frac{\Phi * 10^7}{6.19 * e^{5427/T}}U_\mathrm{T})^2}$$

In above expression, U_ω is the total uncertainty in humidity ratio, U_Φ and U_T is the total uncertainty in the relative humidity and temperature. (Aarnes, 2012).
Similar expression as of Eq. 27 can be written as under:

$$U_{\varepsilon l} = \sqrt{\begin{aligned}&\left(\frac{1}{\omega_{outoor\ air} - \omega_{indoor\ air}}\right)^2 U^2_{\omega\ Supply\ air}\\ &+\left(\frac{\omega_{supply\ air} - \omega_{indoor\ air}}{(\omega_{outoor\ air} - \omega_{indoor\ air})^2}\right)^2 U^2_{\omega\ outdoor\ air}\\ &+\left(\frac{\omega_{outdoor\ air} - \omega_{supply\ air}}{(\omega_{outoor\ air} - \omega_{indoor\ air})^2}\right)^2 U^2_{\omega\ indoor\ air}\end{aligned}} \qquad Eq.28$$

Eq. 28 was used to calculate the total uncertainty in latent effectiveness. In Eq. 28 $U_{\varepsilon l}$ is the total uncertainty in the latent effectiveness, $U_{\omega\ supply\ air}, U_{\omega\ outdoor\ air}\ and,\ U_{\omega\ indoor\ air}$ is the total uncertainty in the humidity ratio of the supply air, outdoor air and the indoor air, $\omega_{outdoor\ air},\ \omega_{indoor\ air},\ and\ \omega_{supply\ air}$ is the humidity ratio of outdoor air, indoor air and supply air in $[kg_{water}/kg_{dry\ air}]$ respectively.

Table 2 shows the mean values, standard deviation, random uncertainty, systematic uncertainty and the total uncertainty of measured quantities.

Table 2 Parameters used to calculate the uncertainty in effectiveness

		Indoor air		**Outdoor air**		**Supply air**		**Exhaust air**	
		RH %	T °C	RH %	T °C	RH %	T °C	RH %	T °C
Mean value	x_{avg}	16.60	18.16	68.51	-12.90	16.56	12.08	65.17	-5.47
Standard deviation	σ	0.4392	0.0401	0.9725	0.0291	0.8946	0.0314	0.4254	0.0210
Random uncertainty	U_r	0.1660	0.0151	0.3675	0.0110	0.3381	0.0118	0.1608	0.0079
Systematic uncertainty	U_s	2	0.2	2	0.2	2	0.2	2	0.2
Total uncertainty	U_T	2.0069	0.2005	2.0335	0.2003	2.0283	0.2003	2.0064	0.2001
Total uncertainty	U_ω	7.9×10^{-06}		2.3×10^{-06}		3.9×10^{-06}			

	ε_s Sensible effectiveness	**ε_l Latent effectiveness**	**ω indoor air (kg_w/kg_{da})**	**ω outdoor air (kg_w/kg_{da})**	**ω supply air (kg_w/kg_{da})**
x_{avg}	0.80	0.40	0.0021	0.0009	0.0014
U	0.0083	0.0045	7.9×10^{-06}	2.3×10^{-06}	3.9×10^{-06}

Leakage tests

Before actual measurements, it was necessary to know the leakages in the system, especially in the test chamber. To avoid leakages, the top lid of the test rig was sealed. The sealing was applied between the test rig and the top lid as well as between the walls of the compartment and the top lid. Likewise, a sealing was also applied between the floor of the test rig and the bottom of the heat exchanger.

Internal leakages

Leakage tests were performed according to the European standard of testing heat and enthalpy exchanger (DS/EN308)

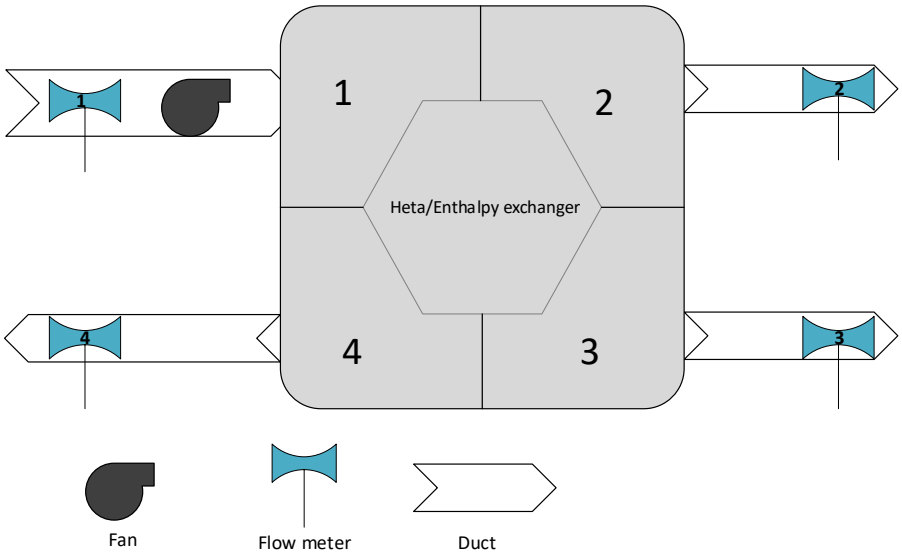

Figure 16 Schematic of internal leakage test setup

To analyse the internal leakage from compartment 1 as shown in Figure 16, a fan was installed at the inlet of compartment 1. The heat exchanger face at compartment 3 was sealed with the tap so that there was no flow through heat exchanger between compartment 1 and 3. Compartment 1 was pressurized and depressurized up to ± 500 Pa. Afterward sealing at the contact of compartment walls and heat exchanger was improved and the test was repeated twice. The reading of Flow meter 2, 3 and 4 was the leakage from compartment 1 to 2, 3 and 4 respectively. The difference in Flow meter 1 and the sum of remaining 3 flow meters was the leakage between compartment 1 and outside of the test chamber. The same procedure was adapted to the remaining three compartments. The internal leakage test must be repeated whenever another heat exchanger is tested.

External Leakages

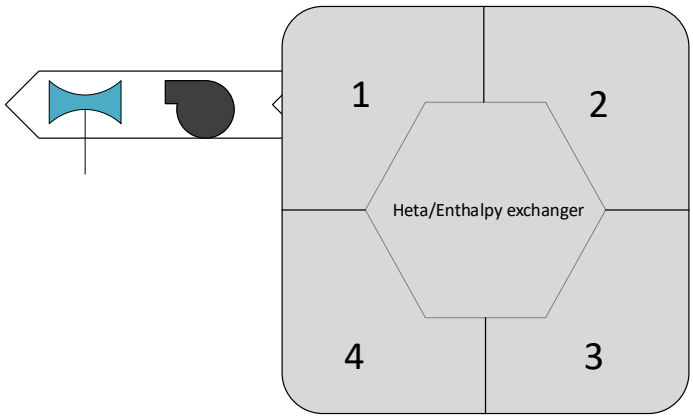

Figure 17 Schematic of external leakage test setup

External leakage was obtained by sealing all the outlets other than one. The air pressure up to ± 500 Pa is applied and airflow rate was measured, see Figure 17.

Results

Internal and external leakage

Before starting the measurements, internal and external leakage tests to check the leakage in the test rig was done as mentioned in the previous chapter. During the tests, it was observed that there was no internal leakage in the test rig. However, a small leakage in the external leakage tests was observed which is shown in Figure 18 and Figure 19.

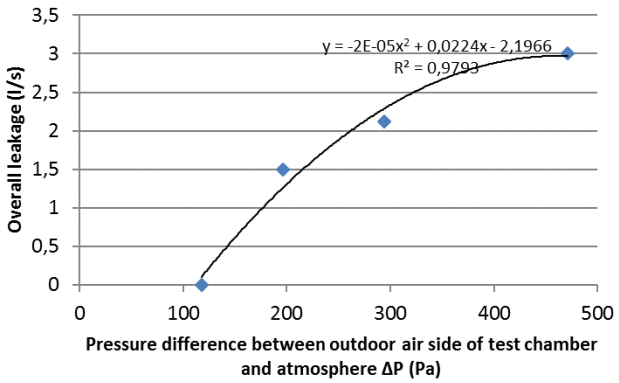

Figure 18 External leakage at outdoor airside of test chamber

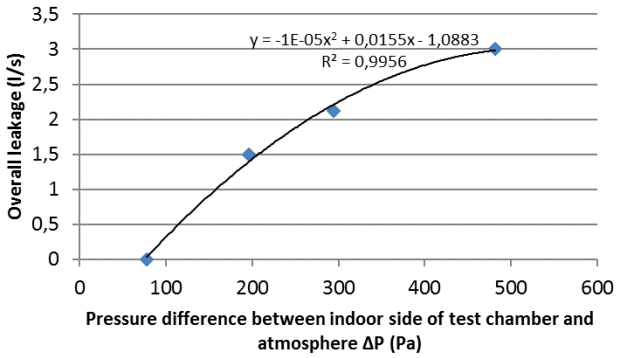

Figure 19 External leakage at indoor airside of test chamber

Short-term performance analyses

Short-term studies were performed to analyse thermal and enthalpy performance of one heat and four enthalpy exchangers under different operating conditions. e.g. outdoor air temperature and face velocities.

Influence of outdoor air temperature on effectiveness

Experiments were performed to analyse the influence of outdoor air temperature on effectiveness at constant airflow. The outcomes of these short-term tests are shown in Figure 20. The notations HX1, EX1, EX2, EX3 and EX4 stands for heat exchanger 1, enthalpy exchanger 1, 2, 3, and 4 respectively. εs, εl, and εt, stands for sensible, latent and total effectiveness respectively.

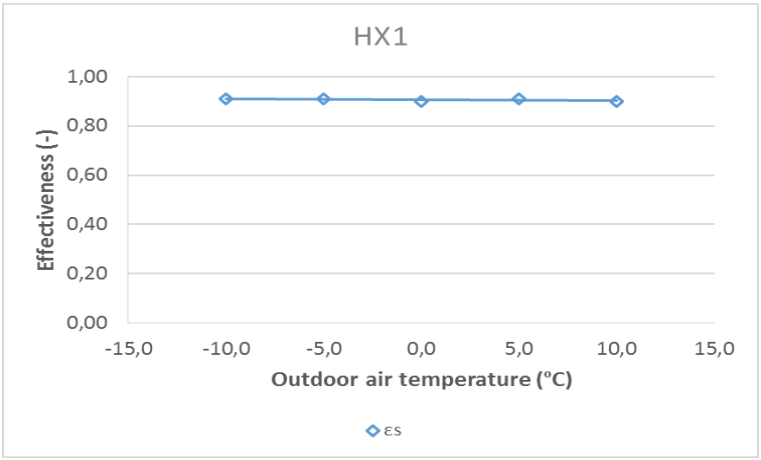
HX1
1,00
0,80
0,60
0,40
0,20
0,00
Effectiveness (-)
-15,0
-10,0
-5,0
0,0
5,0
10,0
15,0
Outdoor air temperature (°C)
εs

(a)

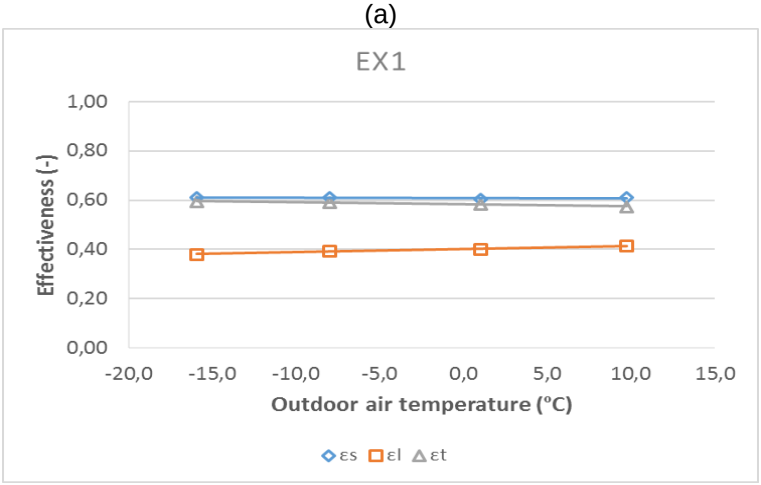
EX1
1,00
0,80
0,60
0,40
0,20
0,00
Effectiveness (-)
-20,0
-15,0
-10,0
-5,0
0,0
5,0
10,0
15,0
Outdoor air temperature (°C)
εs
εl
εt

(b)

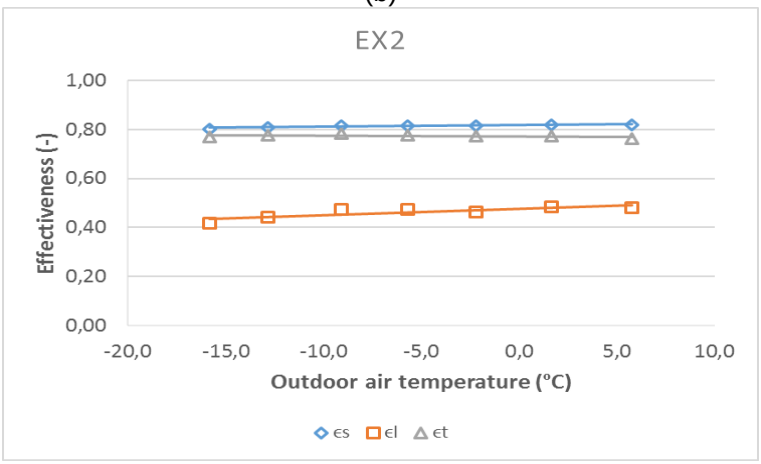
EX2
1,00
0,80
0,60
0,40
0,20
0,00
Effectiveness (-)
-20,0
-15,0
-10,0
-5,0
0,0
5,0
10,0
Outdoor air temperature (°C)
εs
εl
εt

(C)

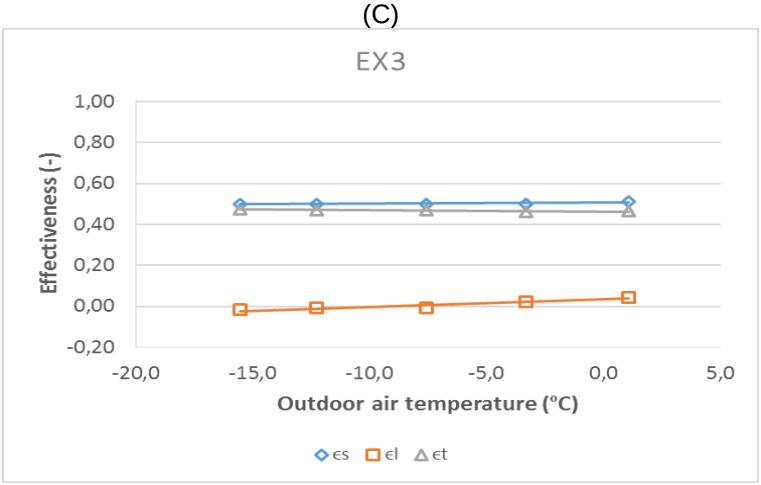
EX3
1,00
0,80
0,60
0,40
0,20
0,00
-0,20
Effectiveness (-)
-20,0
-15,0
-10,0
-5,0
0,0
5,0
Outdoor air temperature (°C)
εs
εl
εt

(d)

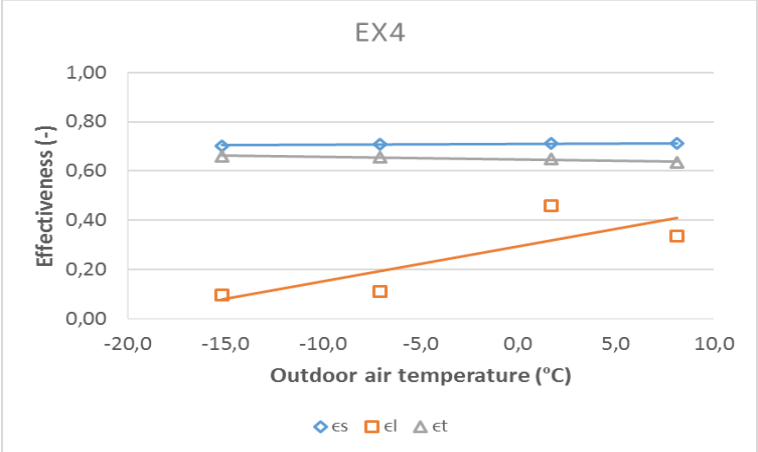

(e)

Figure 20 Variation in effectiveness with outdoor air temperature. εs, εl, and εt stands for sensible, latent and total effectiveness respectively.

The HX1 was a sensible heat exchanger, which was analysed for 48 hours. Eq. 15 was used to calculate the sensible effectiveness. Indoor air during the measurements was kept at constant conditions of 20°C and 50 % relative humidity.

EX1 was analysed at different outdoor air temperatures and constant airflow rates for 40 hours. The sensible, latent and the total effectiveness was calculated using Eq. 15, 16 and 17. The average values of the sensible, latent and the total effectiveness at each temperature was used to observe the influence of the outdoor air temperature on the effectiveness.

EX2 was analysed at different outdoor air temperatures and constant airflow rates for 190 hours. The experiment was performed at five different outdoor air temperatures. Average of 38 hours of data at each temperature was used to calculate and analyse the sensible, latent and total effectiveness. Data was retrieved when the temperature was reached at the set point for each set of measurements.

EX3 was analysed at five different temperatures. Individual measurements at each temperature were carried out in order to calculate the effectiveness. Data retrieval was started when the temperature was reached at the desired level. The experiment was performed at each temperature for 5 hours. Average data of five hours for each temperature was used to observe the effect.

EX4 was analysed for 120 hours at four different temperatures and constant airflow rate. Average data for 30 hours at each outdoor air temperature was used to calculate the effectiveness.

Influence of face velocity on effectiveness

Experiments were performed to analyse the influence of face velocity on the sensible effectiveness of HX1, and the influence of face velocity on the sensible, latent, and the total effectiveness of enthalpy exchangers EX1, EX2, EX3 and EX4.

The results are shown in Figure 21. The results show that the sensible effectiveness of HX1 and the sensible, latent and total effectiveness of EX1, EX2, EX3, and EX4 are varying with face velocity.

Effectiveness was calculated at different face velocities at constant temperature (for each experiment). One hour data with a time interval of 10 minutes was used for each face velocity. The average of each hour's data was used to assess the influence.

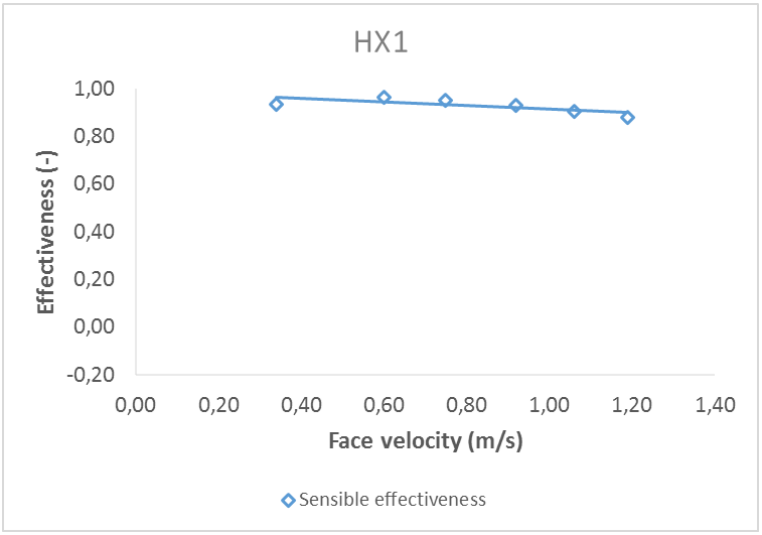
HX1
1,00
0,80
0,60
0,40
0,20
0,00
-0,20
Effectiveness (-)
0,00
0,20
0,40
0,60
0,80
1,00
1,20
1,40
Face velocity (m/s)
Sensible effectiveness

(a)

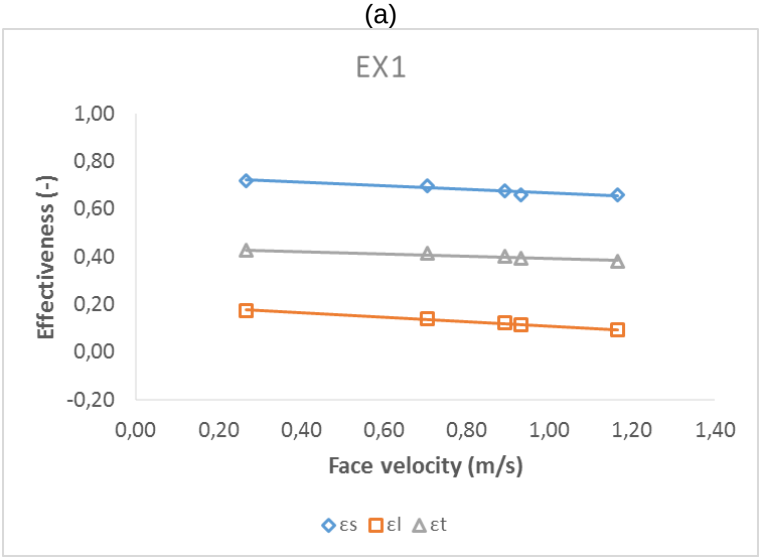
EX1
1,00
0,80
0,60
0,40
0,20
0,00
-0,20
Effectiveness (-)
0,00
0,20
0,40
0,60
0,80
1,00
1,20
1,40
Face velocity (m/s)
εs
εl
εt

(b)

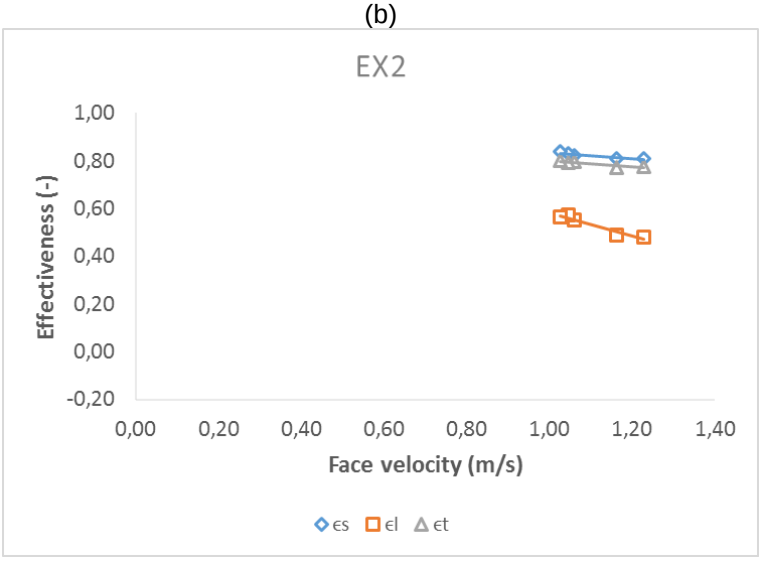
EX2
1,00
0,80
0,60
0,40
0,20
0,00
-0,20
Effectiveness (-)
0,00
0,20
0,40
0,60
0,80
1,00
1,20
1,40
Face velocity (m/s)
εs
εl
εt

(c)

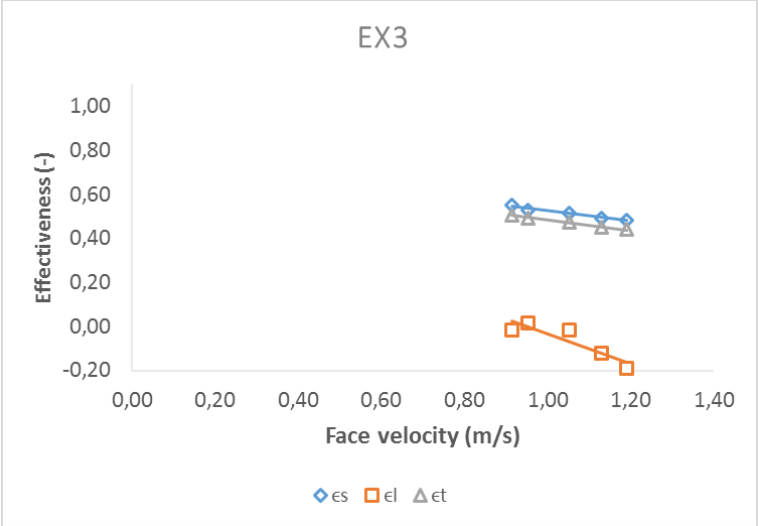

(d)

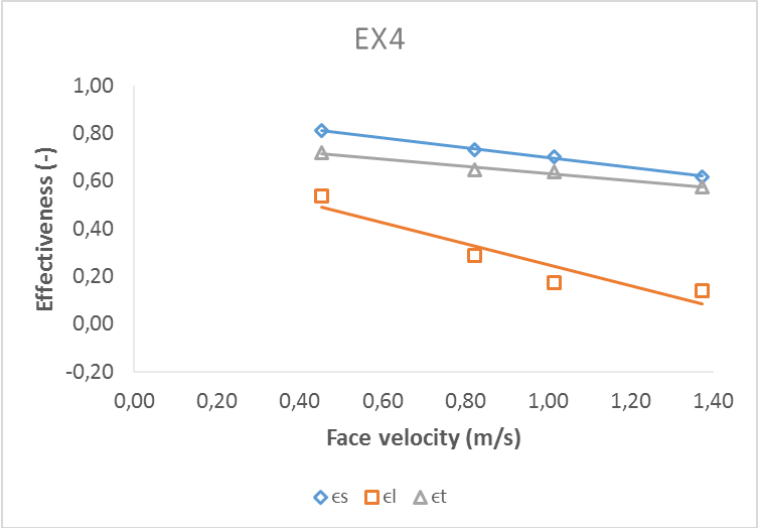

(e)

Figure 21 Variation in effectiveness with face velocity. ɛs, ɛl, and ɛt stands for sensible, latent and total effectiveness respectively.

Long-term performance analyses

To analyse the performance of enthalpy exchanger, an experimental study was performed for a period of two months. Based on the short-term study, EX2 was selected for the long-term performance. The aim of this experiment was to clarify if there was any influence of outdoor air temperature and face velocity on the performance of enthalpy exchanger. The parameters used during the experiment are shown in the Table 3.

Table 3 Parameters used for long-term performance of EX2

Measured outdoor air temperature (ºC)	Measured outdoor air relative humidity (%)	Duration of test (h)	Measured airflow rate (m^3/s)
-16	60	120	0.10
-12	65	140	0.10
-9	70	160	0.10
-5	73	220	0.10
-2	77	220	0.10
2	80	220	0.10
5	82	220	0.10

The influence of outdoor air temperature on the sensible, latent, and total effectiveness was recorded.

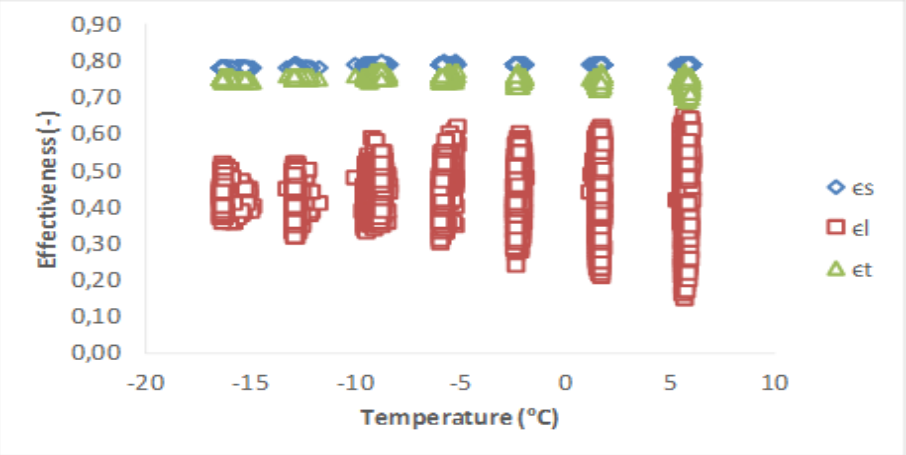

Figure 22 Influence of outdoor air temperature on effectiveness for long-term performance test. ɛs, ɛl, and ɛt stands for sensible, latent and total effectiveness respectively.

Figure 22 shows the long-term heat and enthalpy performance of EX2 in terms of sensible, latent and total effectiveness. Data of temperature, relative humidity, flow rate, and, atmospheric pressure was collected and analysed to calculate sensible, latent, and, total effectiveness at different outdoor air temperatures as shown in Table 3. The water content in the inlet air varies because of the variation in outdoor relative humidity. The average value calculated for latent effectiveness at different temperatures varies between 0.43 and 0.47 with an average of 0.45.The maximum and minimum value for the latent effectiveness were 0.65 and 0.15 respectively. However, it can be assumed that the latent and total effectiveness varies but there is a very little effect of outdoor air temperature on overall latent effectiveness. 78 % to 79 % sensible, 15 % to 65 % latent, and 68 % to 77 % total effectiveness was calculated.

Similarly, the influence of face velocity on the sensible, latent, and the total effectiveness was observed. Figure 23 shows the influence of face velocity on effectiveness. The results show that the sensible, latent and total effectiveness are varying with face velocity. The linear trend lines show the inverse relation between face velocity and effectiveness. Effectiveness was calculated at five different face velocities at constant temperature (for each experiment). One hour data with a time interval of 10 minutes was used for each face velocity. The average of each hour's data was used to evaluate the influence. Results of two experiments at different temperatures are shown in Figure 23.

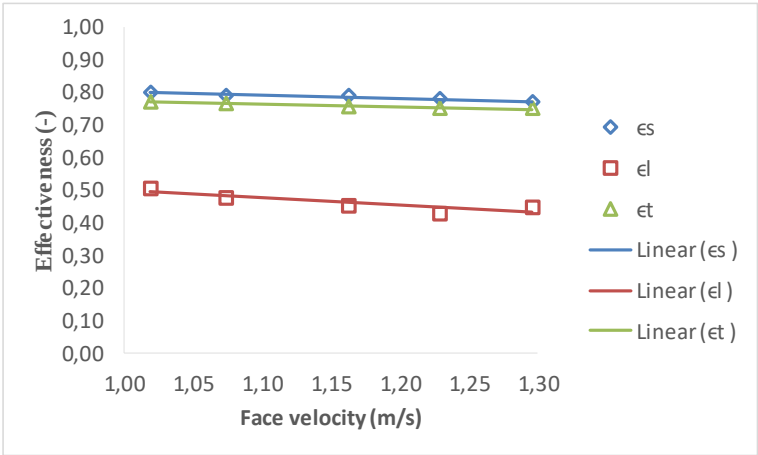

(2a) At -16 ºC

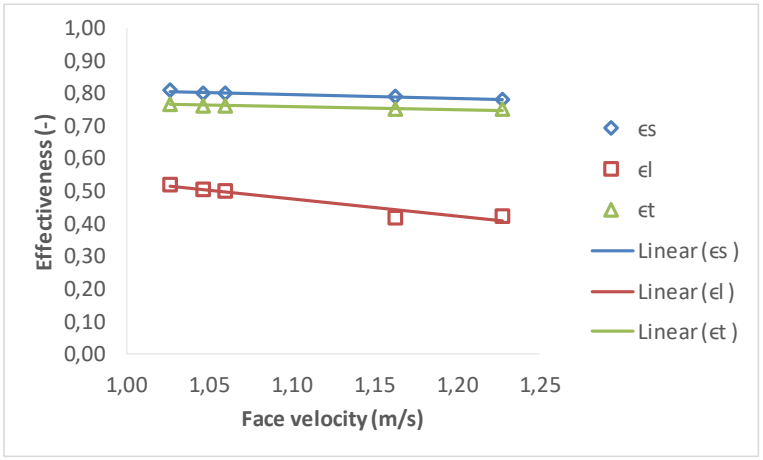

(2b) At -2 ºC

Figure 23 Influence of face velocity on effectiveness after long-term performance of the exchanger. ɛs, ɛl, and ɛt stands for sensible, latent and total effectiveness respectively.

Performance of EX2 in terms of energy transfer rate.

Figure 24 shows the performance of the enthalpy exchanger in terms of energy transfer rate. A comparison was carried out between actual energy recovered and maximum possible energy recovery. As an example: at -16 ºC outdoor air temperature, 3.5 kW energy was recuperated out of 4.5 kW. Here, 3.5 kW is the actual recovered energy and 4.5 kW is the maximum possible recoverable energy. In terms of percentage, 78 % total energy was recuperated at -16 ºC. Here it is relevant to mention that, sensible energy contributed 95 % of the enthalpy recovered and latent energy contributed about 5 %. In the whole process of measurement, (from -16 ºC to 5 ºC) it was observed that the major part of the recovered energy was consists of the sensible part which is 88 % to 95 %. However, 5 % to 12 % of enthalpy energy was recuperated from the latent part which is wasted in the sensible heat exchanger. In addition, it can also be concluded that the latent effectiveness increases slightly with the increase in temperature; however, there is no major contribution of the increase in latent energy in the recuperated enthalpy.

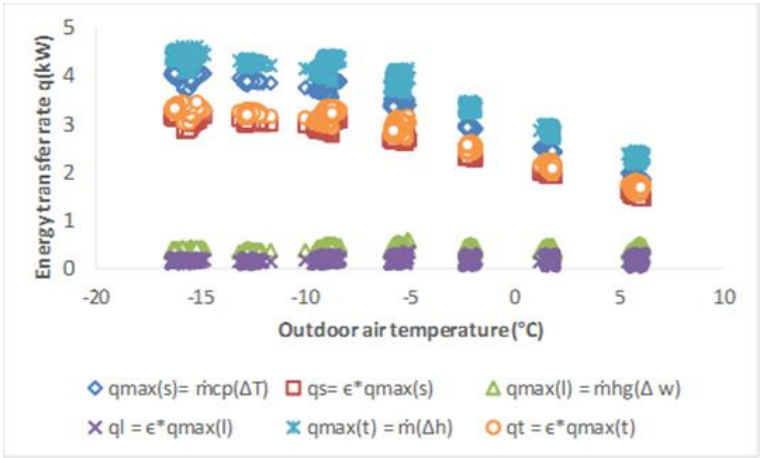

Figure 24 Performance in terms of energy transfer ratio

Uncertainty

Statistical uncertainties in sensible and latent effectiveness was calculated based on measured data. The parameters used to calculate the uncertainty are shown in Table 2. Total uncertainty in sensible effectiveness and latent effectiveness was 8.3 % and 4.5 % respectively with 95 % confidence level.

N_2O gas transfer

Experiments were performed in order to investigate the transfer of N_2O gas molecules through the membrane of enthalpy exchangers. EX2 and EX4 were selected and used for this purpose. Eq.23 was used to calculate the N_2O transfer ratio.

Influence of outdoor air temperature

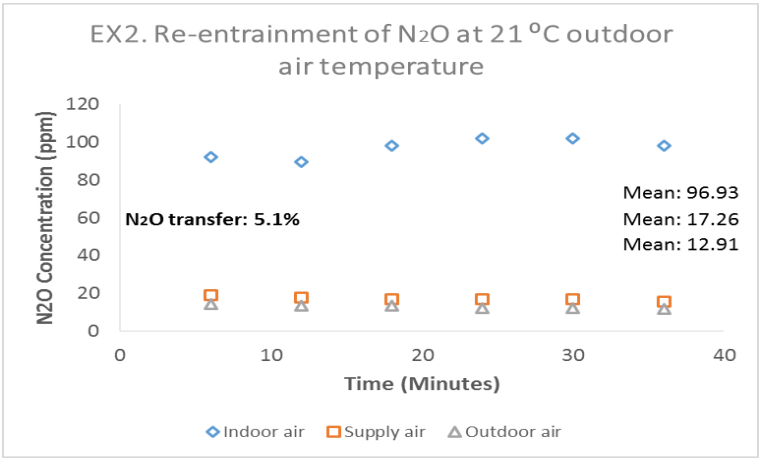

(a)

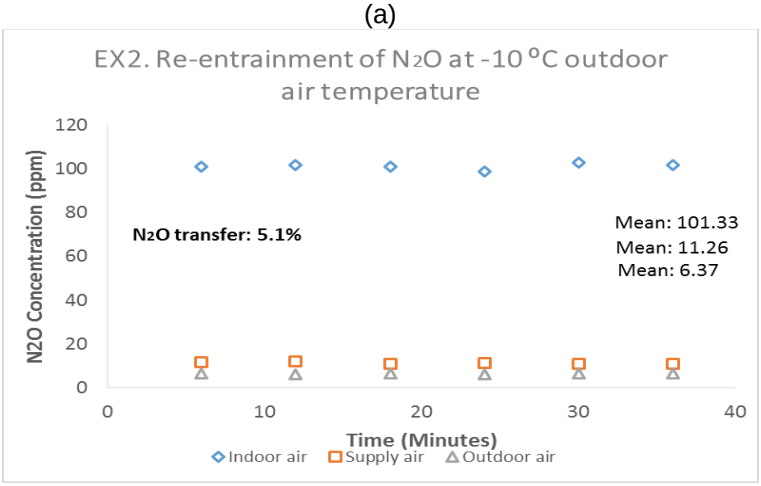

(b)

Figure 25 Influence of outdoor air temperature on N_2O transfer through polymer membrane

N_2O concentration was measured at outdoor airside, supply airside and indoor airside. The experiments were performed at two different temperatures (21 ºC and -10 ºC) to observe if there is any influence of outdoor air temperature on the transfer of N_2O through the membrane. The results showed that there was no influence of outdoor air temperature on the N_2O transfer through the polymer membrane. 5.1 % N_2O was transferred through the membrane of EX2.

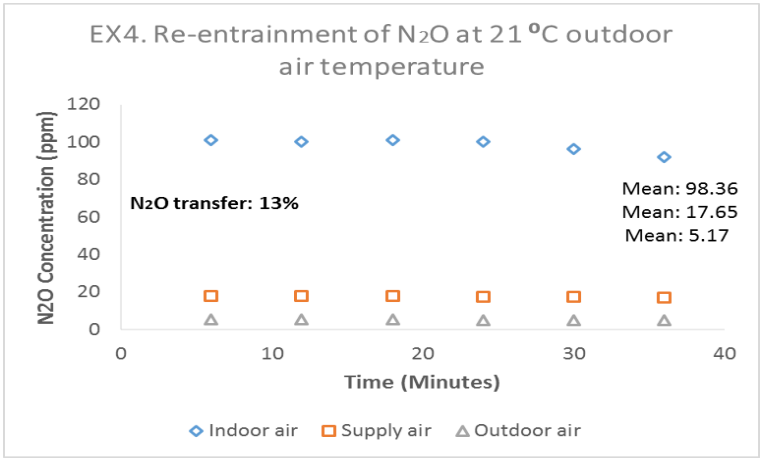

(a)

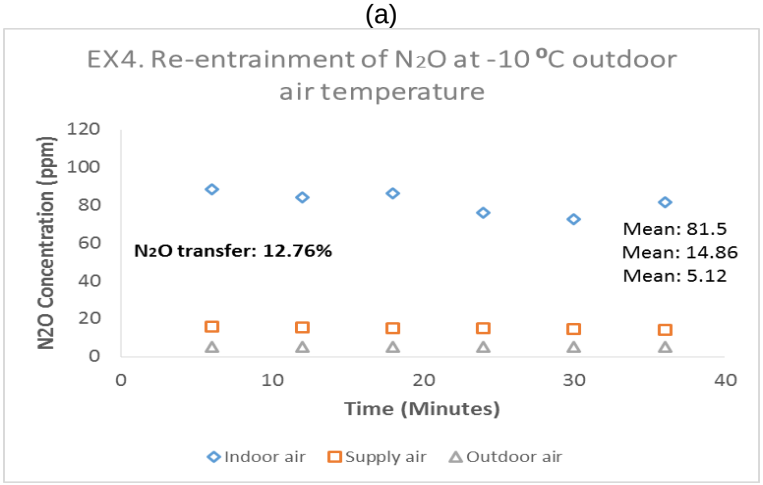

(b)

Figure 26 Influence of outdoor air temperature on N_2O transfer through treated paper membrane

Similar experiments were performed for EX4. The results are shown in Figure 26. The results showed that there was negligible influence of outdoor air temperature on the transfer of N_2O gas molecules through treated paper membrane. About 13 % N_2O gas transfer was calculated based on measured data.

Influence of N_2O concentration on transfer

Experiments were performed to study the influence of N_2O concentration on transfer ratio through the polymer membrane and treated paper membrane.

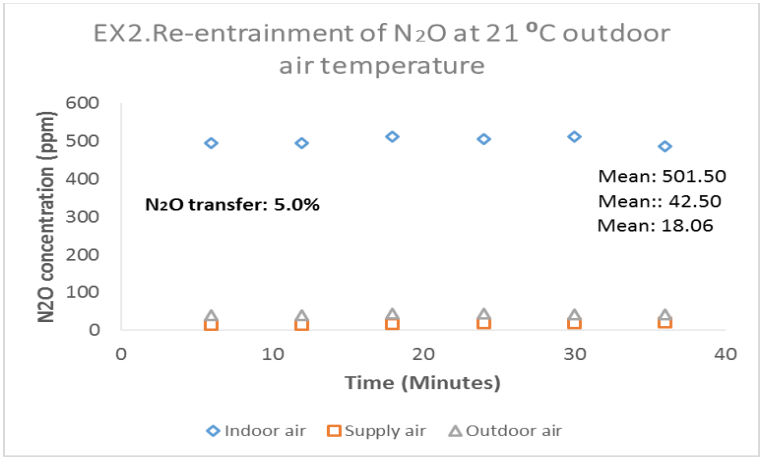

(a)

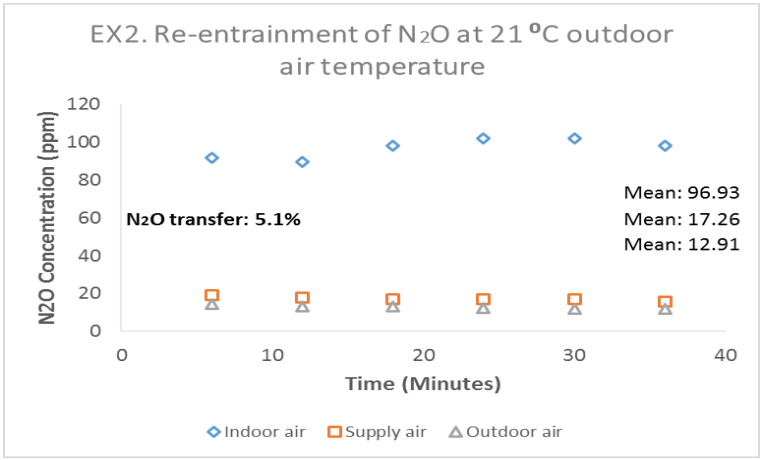

(b)

Figure 27 Influence of N_2O concentration on transfer through polymer membrane

Figure 27 shows the results of the influence of N_2O concentration on the transfer ratio. EX2 was studied for N_2O gas transfer through the membrane at different concentration levels. The results showed that there was almost no influence of gas concentration on transfer through the membrane.

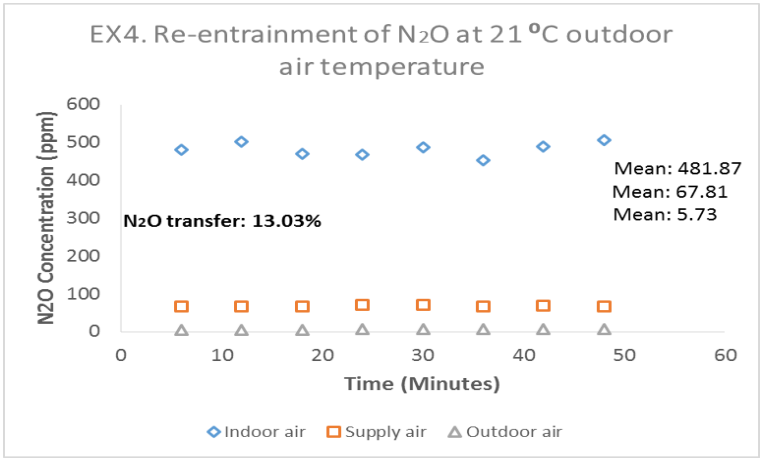

(a)

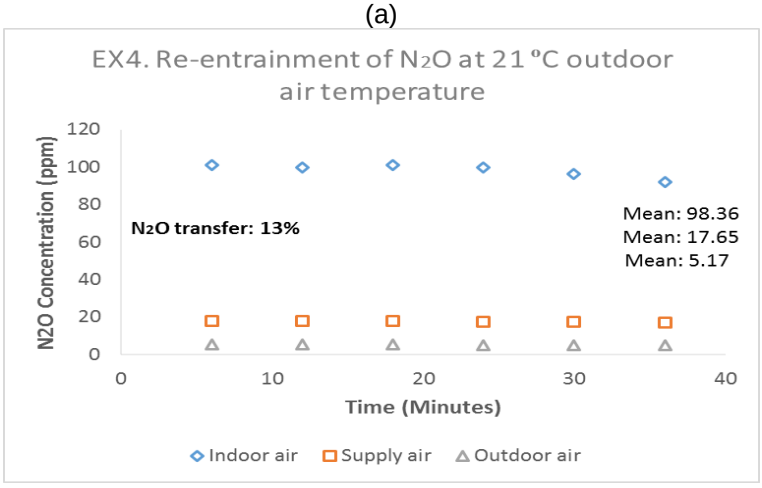

(b)

Figure 28 Influence of N_2O concentration on transfer through treated paper membrane

Similar experiment was performed with EX4 to analyse the influence of N_2O concentration on the transfer ratio through treated paper membrane. Figure 28 shows the experimental results for EX4. The N_2O concentration at indoor air terminal was increased to observe the influence of concentration on transfer ratio. It was observed that there was no influence of concentration of N_2O on the transfer ratio of gas molecules through the treated paper membrane.

Frost formation

An experiment was performed in order to investigate the risk of ice accretion on the fins of the heat exchanger. In this experiment, the operating conditions e.g. outdoor air temperature and relative humidity of the outdoor air were kept constant. i.e. at -16 ºC and 80 % RH respectively. The pressure drop at supply and exhaust side was measured in the beginning and after passing 20 hours. It was observed that there was no change in the pressure difference on supply and exhaust side which could be an indication of frost free operation of enthalpy exchanger.

Similar experiments were performed for all the enthalpy exchangers and no frost formation was observed on any of them.

Deformation in the membrane

In N_2O gas transfer analyses, it was observed that there was no influence of outdoor air temperature on the transfer of N_2O molecules. The gas concentration transfer ratio remained unchanged for different outdoor air temperatures. From these results, it can be assumed that the treated paper membrane and polymer membrane have rigid behaviour against temperature and no deformation/crumpling in the membranes could be expected. It should be noted that the deformation in the membrane was not visible with naked eye.

Discussion

The objective of this study was,

- To analyse the thermal and enthalpy performance of heat and enthalpy exchangers under different operating conditions,
- To analyse the N_2O gas transfer through the polymer and paper based membrane under different parameters,
- To investigate the ice formation in the enthalpy exchanger, and
- To investigate the deformation/crumpling in the membrane of enthalpy exchangers under different operating conditions.

In this study, one air-to-air heat exchanger and four air-to-air enthalpy exchangers were studied and the results were analysed. The sensible heat exchanger was capable of transferring only heat energy while enthalpy exchangers were capable of transferring not only heat energy but also the moisture/latent energy from stale air to the outdoor air.

Performance in terms of thermal and enthalpy effectiveness

From Figure 20 (a), (b), (c), (d), and (e), it can be seen that all the heat and enthalpy exchangers showed similar behaviour at different outdoor air temperatures i.e. the sensible effectiveness was almost independent of outdoor air temperature. These results are in agreement with (Zhong et al., 2014; Niu and Zhang, 2001; Liu et al., 2016).

Enthalpy exchangers EX1, EX2, EX3, and EX4 showed that the latent and the total effectiveness were sensitive to outdoor air temperature. The enthalpy energy declines a little with increase in the outdoor air temperature, which is in agreement with (Nie et al., 2015). The latent effectiveness increased with the increase in the outdoor air temperature. The reason of increase in the latent effectiveness is, with the increase in the outdoor air temperature, the average kinetic energy of the water molecules increase and the more molecules collide with membrane, which cause increase in the latent effectiveness (Liu et al., 2016). Moreover, the latent effectiveness also depends on the membrane properties and outdoor air conditions like temperature and relative humidity (Niu and Zhang, 2001; Zhang et al., 2008). However, the results regarding the relation between outdoor air temperature and latent effectiveness opposed the results reported by (Niu and Zhang, 2001)

The analysis of the results of sensible heat exchanger HX1 showed that the sensible effectiveness was a function of face velocity. Increase in the face velocity, caused decrease in sensible effectiveness. Similarly, enthalpy exchangers EX1, EX2, EX3 and EX4 showed that the sensible, latent and total effectiveness were functions of face velocity. There is inverse relation between face velocity and effectiveness (sensible, latent and total). The reason is that, by increasing the face velocity, pressure drop increase, resulting in decrease in overall heat and mass transfer coefficient, consequently the number of transfer unit decrease, thus sensible, latent and total effectiveness decrease (Niu and Zhang, 2001).

Figure 29 shows the relation between the face velocity and the change in pressure drop across the enthalpy exchanger. These results are in agreement with (Liu et al., 2016; Nasif et al., 2012; Zhong et al., 2014).

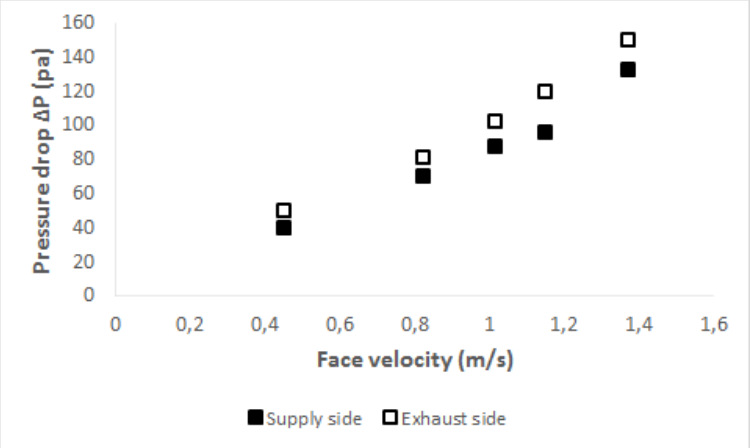

Figure 29 Increase in the pressure drop across the enthalpy exchanger with the increase in the face velocity

Performance in terms of gas transfer through the membrane

N_2O transfer through polymer membrane and treated paper membrane was studied. The experiments were conducted under different parameters. The influence of outdoor air temperature and gas concentration on the transfer rate of N_2O through the membrane were investigated. 13 % N_2O transferred through treated paper membrane and 5 % N_2O transferred through polymer membrane. The high transfer rate of N_2O through the treated paper membrane could be because of properties of paper membrane as researchers have reported that, the transfer rate of moisture through the membrane depends on the properties of the membrane. The same analogy can be assumed. Different materials have different pore sizes, so the porosity of different materials is different.

Figure 25 and Figure 27 shows that 5 % N_2O was transferred from indoor air to the outdoor air through polymer membrane. About 5.4 % to 9 % contaminants transfer through polymer membrane were reported by (Nie et al., 2015) which is one third of what was observed in the absorption rotary enthalpy exchangers studied by (Khoury et al., 1988; Hult et al., 2014).

Our analyses regarding gas transfer is in contradiction with (Hult et al., 2014) in terms of influence of outdoor air temperature on transfer rate of gas molecules. According to the (Hult et al., 2014), the transfer rate of contaminants decreases with the increase in the outdoor air temperature. Our analyses showed that there is no influence of outdoor air temperature on the transfer rate. According to (Nie et al., 2015), the gas transfer ratio is not a function of water solubility or molecular size of the chemical.

Performance analyses in terms of ice accretion

The experiment was carried out for more than 20 hours to study the ice accretion on the fins of enthalpy exchanger. At the beginning of the experiment and after passing 20 hours, the pressure drop was measured across the supply and exhaust airside of enthalpy exchanger. It was observed that there was no change in the pressure drop as well as in the sensible, latent and total effectiveness at same operating conditions(-16 ºC and 82 % relative humidity) which could be an indication of frost free operation.

During the experiments, it was observed that the relative humidity of indoor air remained below 25 %. Though, there was humidifier installed in the chamber 2, but unfortunately, it couldn't provide enough water to increase

the relative humidity to experience the frost formation on the enthalpy exchanger. Out of these analyses, it can be assumed that there would be no ice formation on the enthalpy exchanger even at -16 ºC if the relative humidity of indoor air is below 30 % which is agreement with (Liu et al., 2014).

Deformation of the membrane

In the analyses of deformation in the membrane, it was found that there was no influence of outdoor air temperature and concentration of gas on the transfer ratio of gas molecules through the membranes of enthalpy exchangers. The outcomes of the analyses and the visibility of the membrane indicate that there was no deformation in the treated paper membrane and the polymer membrane.

Advantages and disadvantages of membrane material

Table 4 shows that the EX2 has the highest enthalpy and performed best as compared to other enthalpy exchangers at 1m/s face velocity. HX1 has the highest sensible effectiveness. To effectiveness of EX2 is 2% higher than the total enthalpy of HX1.

Table 4 Thermal and enthalpy performance of heat and enthalpy exchangers

	HX1	EX1	EX2	EX3	EX4
Sensible effectiveness	0.90	0.60	0.82	0.50	0.70
Latent effectiveness	-	0.40	0.55	0.01	0.18
Total effectiveness/enthalpy	0.77	0.59	0.79	0.47	0.64

Advantages and disadvantages of using polymer membrane based enthalpy exchangers in contrast to plastic and paper membrane based heat and enthalpy exchangers are:

Advantages of using polymer membrane enthalpy exchanger

- Highest enthalpy transfer as compared to plastic based heat exchanger and paper based enthalpy exchanger
- No visible frost formation was observed during long and short terms performance analyses. There is risk of frost formation on sensible heat exchanger at low temperature e.g. at -20 ºC outdoor air temperature (Liu et al., 2014)
- Moisture transfer from stale air to outdoor air decrease the dryness of the air in the cold climate, resulting in good indoor air environment
- Low (N_2O) transfer ratio as compared to treated paper based membrane
- Maintenance is easy as compared to rotary wheel enthalpy exchanger
- Polymer membrane based enthalpy exchanger is a viable choice in terms of energy saving potential.

Disadvantages of using polymer membrane enthalpy exchanger

- Polymer membrane enthalpy exchangers are not environmentally friendly and could contribute to polymer wastes
- Cross contamination transfer through the polymer membrane is a disadvantage in terms of degrading indoor air quality

Conclusion

Phase 1.

One heat and four enthalpy exchangers were used for short term performance analyses and one enthalpy exchanger was used for long term performance analyses under different operating conditions

- Outdoor air temperature has no influence on sensible effectiveness. However, the latent effectiveness increase insignificantly with the increase in the outdoor air temperature and the total effectiveness declines with the increase in the outdoor air temperature.
- Face velocity is a function of sensible, latent and the total effectiveness. There is inverse relation between face velocity and the effectiveness.
- Polymer membrane enthalpy exchanger showed the highest sensible and enthalpy effectiveness as compared to paper and treated paper membrane enthalpy exchangers.
- Membrane based enthalpy exchanger has 2 % higher enthalpy than the sensible heat exchanger at same face velocity.

Phase 2.

One polymer membrane based enthalpy exchanger and one treated paper membrane based enthalpy exchanger were studied to identify the N_2O transfer through the membrane at different conditions.

- Outdoor air temperature has no influence on the transfer ratio of N_2O through the polymer membrane and treated paper membrane.
- The concentration level of N_2O has no impact on the transfer ratio through the polymer and treated paper membrane.
- Permeation of N_2O through the polymer membrane and the treated paper membrane were 5.1 % and 13 % respectively.

Phase 3.

The third phase of the study was to investigate if frost formation occur under cold climate.

- No pressure drop across the enthalpy exchanger at -16 ºC was observed during 20 hours of testing which indicates that there was no ice formed on the enthalpy exchanger.
- No visible ice formation was observed during long term experiment (120 hours at -16 ºC)

Phase 4.

The study was to identify occurrence of deformation under cold climate.

- It is assumed that there was no deformation in the membrane. The assumption is based on experimental results of N_2O transfer analyses when the experiment was carried out at -10 ºC and 21 ºC.

- No visible deformation was observed in the membranes.
- No change in pressure drop at constant operating conditions could also be an indication of rigidness of the membrane.

Appendix

Calibration/Co-calibration of HCS sensors

In July 2016 two of HCS sensors were calibrated. Remaining HCS sensors were co-calibrated with the calibrated ones. SBi has item numbering on the sensors. The calibrated HCS have the following numbers:

- 4792
- 4702

Remaining HCS were co-calibrated with the above mentioned calibrated sensors. The co-calibration was done as the difference in the measurements between calibrated one and the non- calibrated one. The difference is then defined in terms of percentage with respect to the calibrated one and this percentage is termed as error.

Calibration procedure

10 HCS sensors (including 4792 and 4702) were placed in chamber 2 of the test rig. Then the sensors were exposed to several humidity levels and at least one temperature for co-calibration. 10 HCS sensors were co-calibrated with respect to sensor number 4792 and 4702.

4701

Temperature

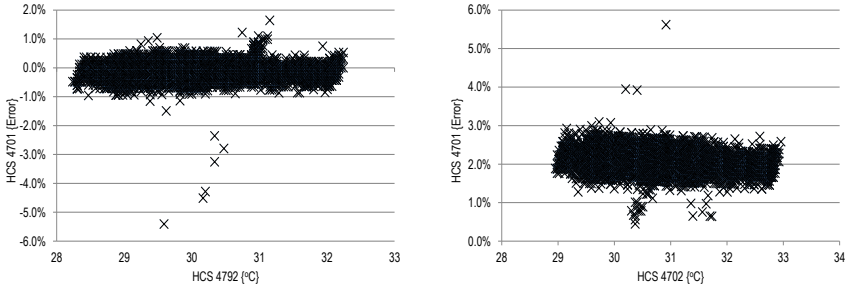

For dry bulb temperatures, the error margin of 4701 was under ±1 % of 4792. However, as an average the 4701 measured 2 % above the value measured by 4702.

Relative humidity

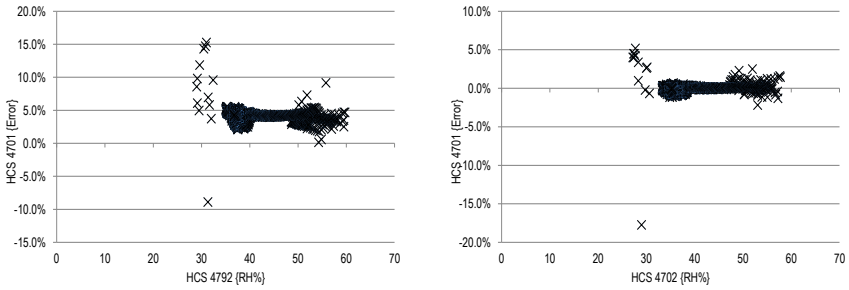

For relative humidity, the error in 4701 was under 5 % of 4792. However, as an average the 4701 measured same value of relative humidity as of 4702.

4702

Temperature

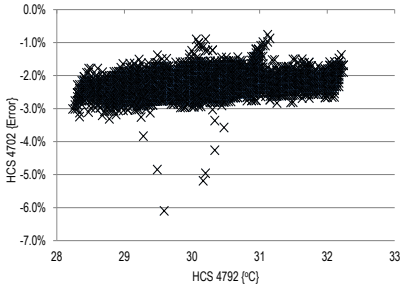

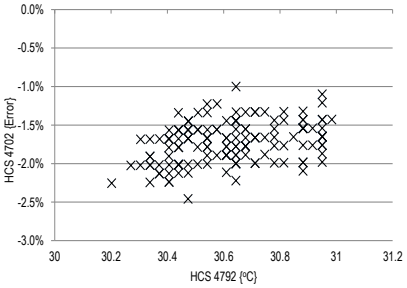

For dry bulb temperatures, the error margin of 4702 was under -3 % of 4792. The experiments were repeated several times with almost similar findings.

Relative humidity

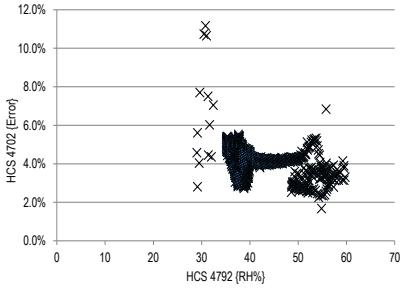

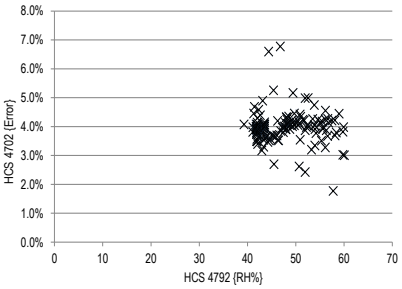

For relative humidity, the error in 4702 was around 4 % of 4792. The experiments were repeated several times with almost similar findings.

4703

Temperature

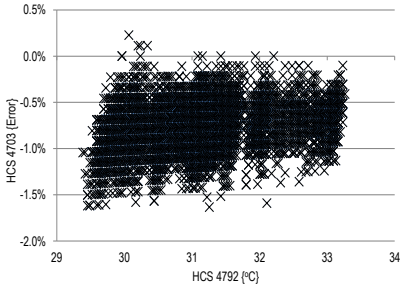

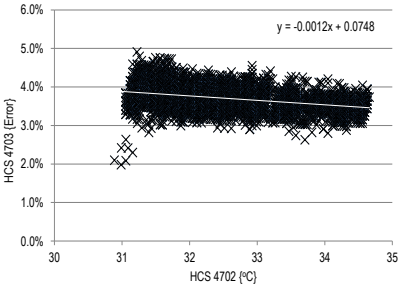

For dry bulb temperatures, the error margin of 4792 was under ±1.5 % of 4792. However, error in 4703 with respect to 4702 can be estimated by a function shown in the above graph.

Relative humidity

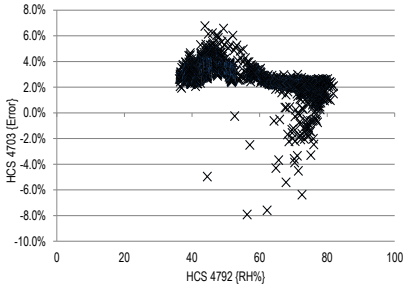

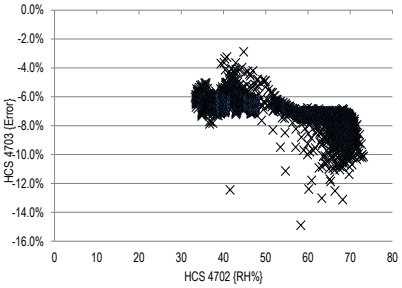

4715

Temperature

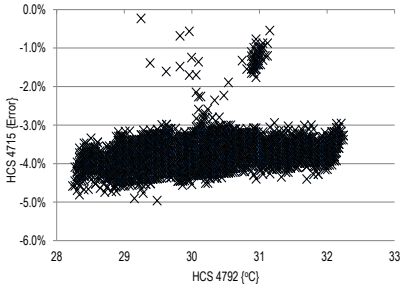

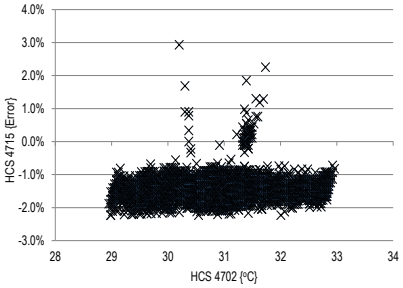

Relative humidity

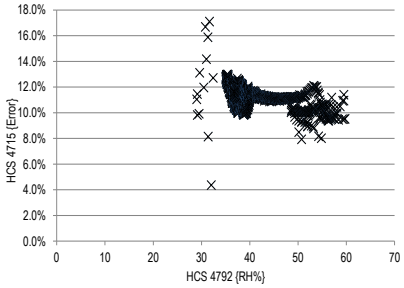

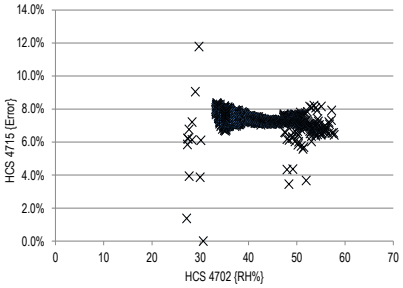

4716

Temperature

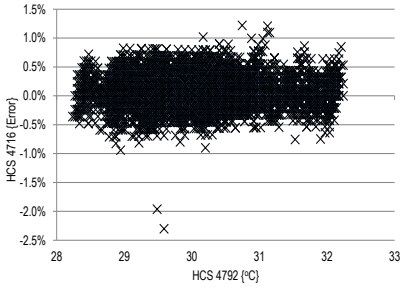

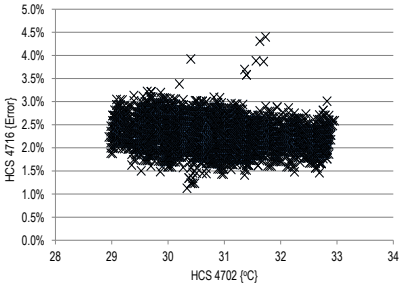

Relative humidity

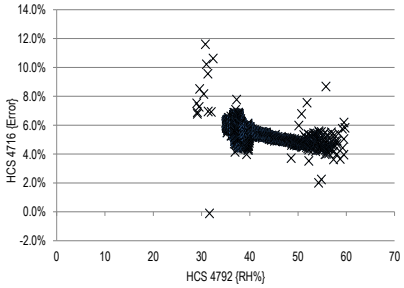

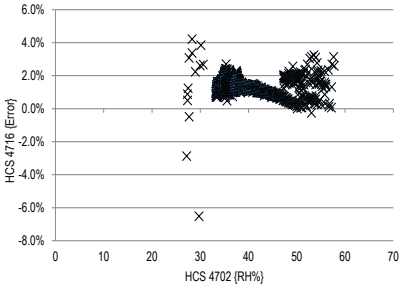

4717

Temperature

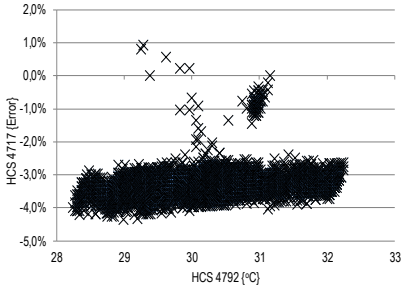

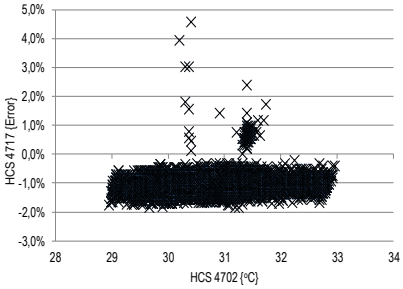

Relative humidity

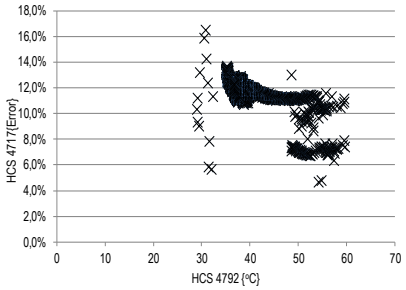

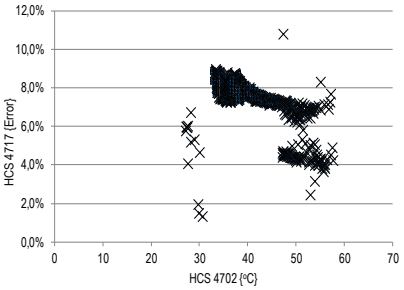

4813

Temperature

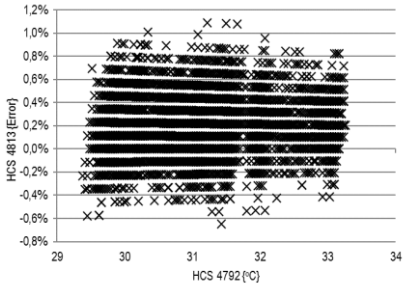

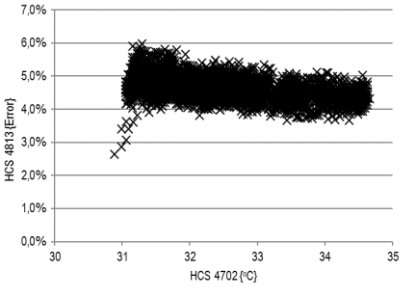

Relative humidity

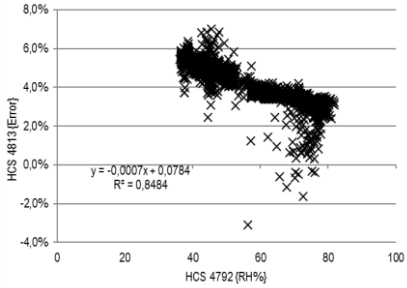

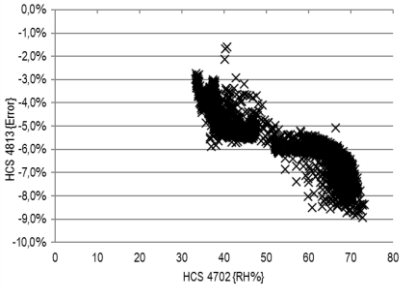

4825

Temperature

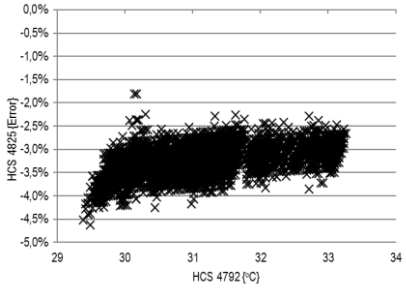

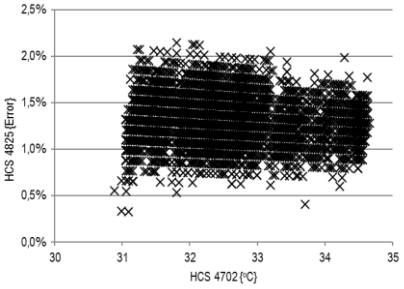

Relative humidity

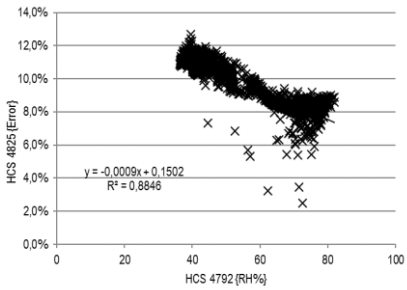

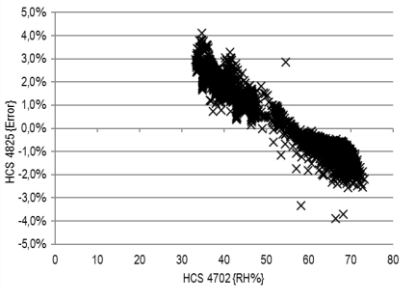

4822

Temperature

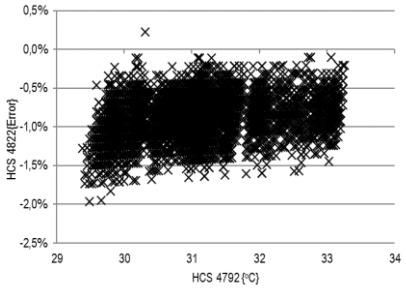

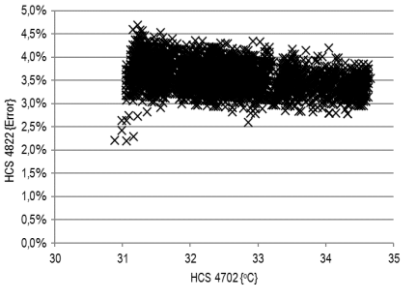

Relative humidity

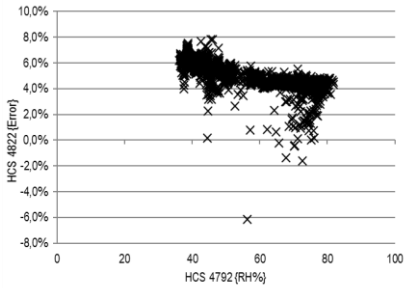

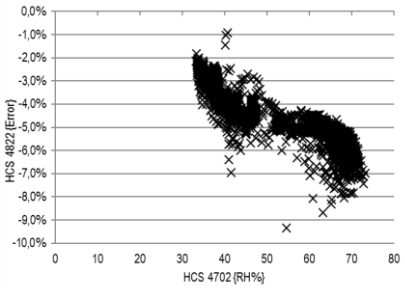

4819

Temperature

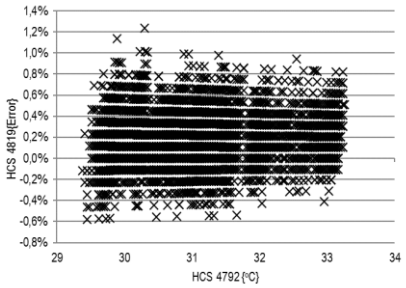

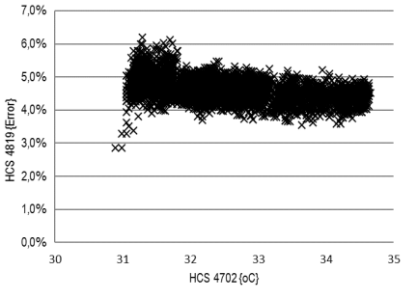

Relative humidity

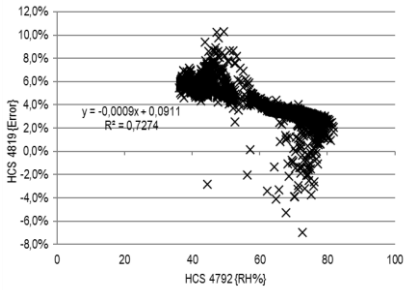

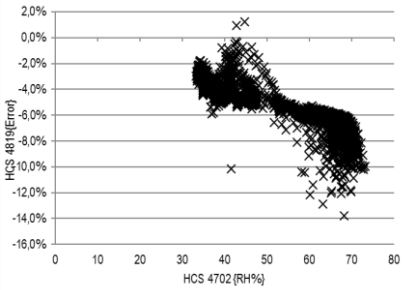

4812

Temperature

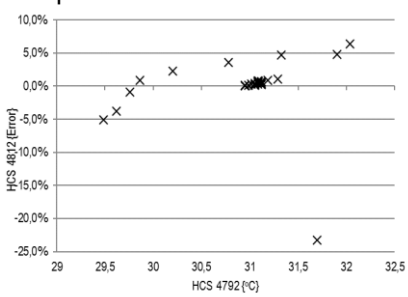

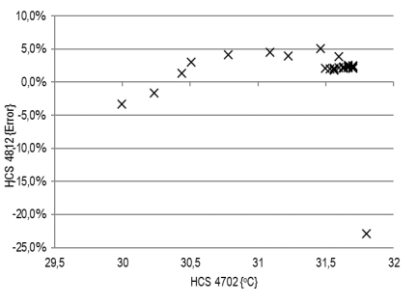

Relative humidity

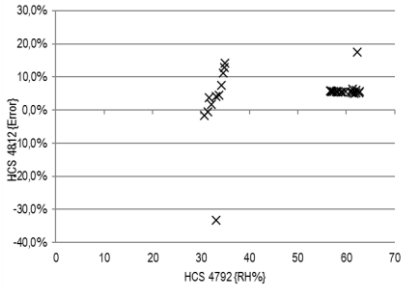

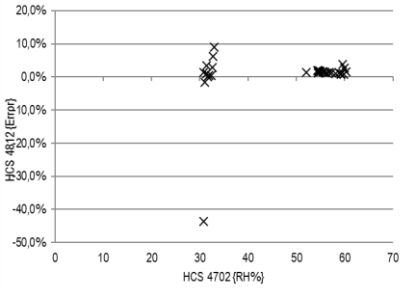

4810

Temperature

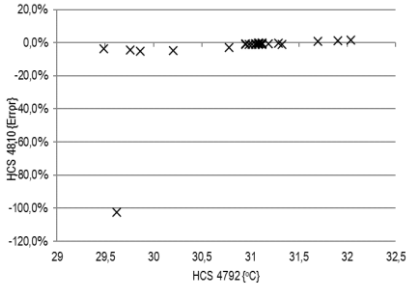

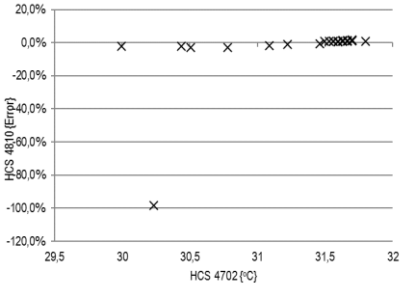

Relative humidity

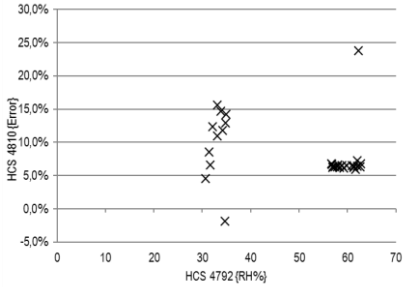

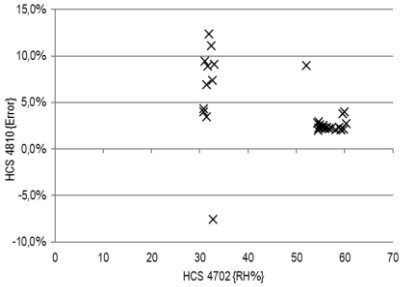

4824

Temperature

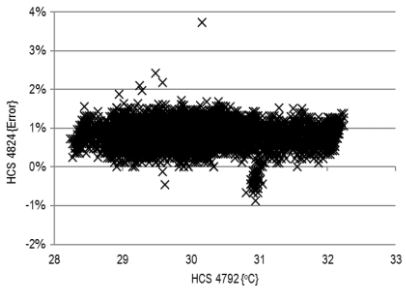

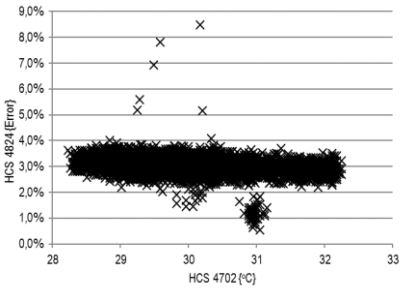

Relative humidity

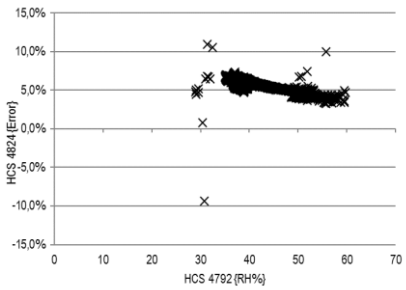

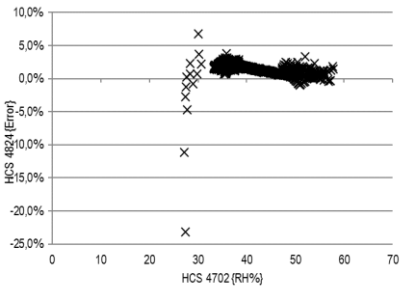

4826

Temperature

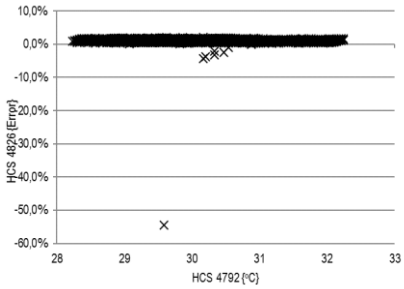

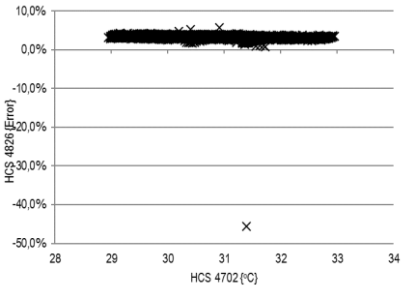

Relative humidity

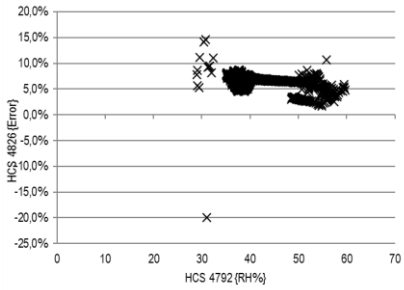

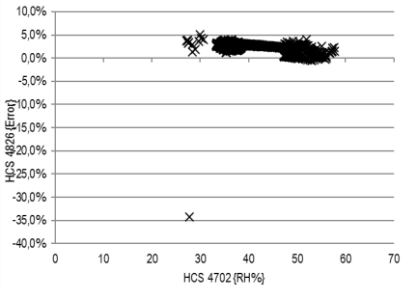

4804

Temperature

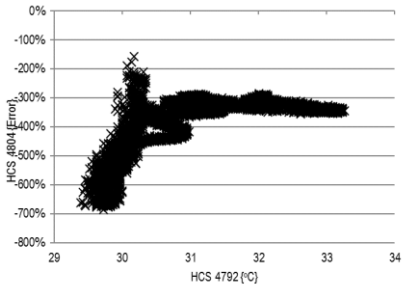

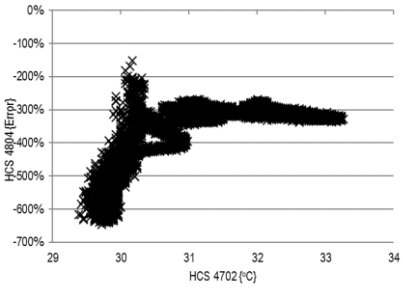

Relative humidity

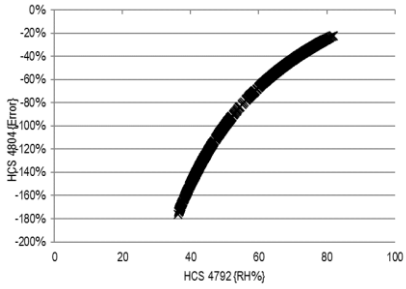

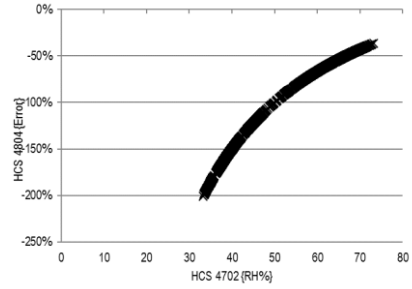

Bibliography

Andersson, B., Andersson,K., Sundell, J., Zingmark, P.A. “Mass Transfer Of Contaminants In Rotary Enthalpy Exchangers.” *Indoor Air*. Helsinki, 1993.

ASHRAE. ANSI/ASHRAE standard 2008-2013, 2008.

DS/EN308. “Heat exchangers - Test procedures for establishing performance of air to air and flue gases heat recovery devices.” 1997.

Farrington R. B., Wells C. V. “A Through Approach to Measurement Uncertainty Analysis Applied to Immersed Heat Exchanger Testing.” *ASME Solar Energy Division Conference*. Anaheim, California, 1986.

Fisk, W. J., Pedersen, B. S., Hekmat,D. C., Raymond, E., and Kaboli, H. *FREEZING IN RESIDENTIAL AIR-TO-AIR HEAT EXCHANGERS:*. Berkeley: Lawrence Berkeley Laboratory, 1985.

Hult E. L., Willem, H., and Sherman, M.H. “Formaldehyde Transfer in Residential Energy Recovery Ventilators.” *Building and Environment,* (2014): 75:92-97.

Khoury, G.A., Chang, S.N., Abdelghani,A.A., and Anderson, A.C. “An investigation of reentrainment of chemical fume hood exhaust air in a heat recovery unit.” *American Industrial Hygiene* (1988): 49(2):61–5.

Kim, A. *Performance of an Air-to-Air Heat Exchanger and an Exhaust Air Heat Recovery Heat Pump*. Ottawa: National research council canada, 1985.

Kistler, K.R., Cussier, E.L. “Membrane modules for building ventilation.” *Chemical Engineering Research and Design* (2002): 53-64.

Liu, P., Maria, J. A., Mathisen, H. M., & Simonson, C. “Performance of a quasi-counter-flow air-to-air membrane energy exchanger in cold climates.” *Energy and buildings* (2016): 129-142.

Liu, P., Maria, J.L., Nasr, M.R., Mathisen, H., & Simonson, C. “Frosting limits for counter-flow Membrane Energy Exchanger (MEE) in cold climates.” *Indoor air quality and climate*. 2014. 488-496.

Nasif, M.S., Waked, R.A., Behnia, M., and Morrison, G. “Modeling of Air to Air Enthalpy Heat Exchanger.” *Heat transfer engineering* (2012): 1010-1023.

Nasr, M.R., Kassai, M., Gaoming, G. , Carey J.S. “Evaluation of defrosting methods for air-to-air heat/energy exchangers on energy consumption of ventilation.” *Applied Energy* (2015): 32-40.

Nie, j., Yang, J., Fang, L., and Kong, X. “Experimental evaluation of enthalpy efficiency and gas-phase contaminant transfer in an enthalpy recovery unit with polymer membrane foils.” *Science and Technology for the Built Environment* 21.2 (2015): 150-159.

Niu J.L., Zhang L.Z. “Membrane-based Enthalpy Exchanger: material considerations and clarification of moisture resistance.” *Journal of Membrane Science* 189 (2001): 179–191.

Robbin, G. S., Stevens, V., Madden, D. *Energy Recovery Ventilators in Cold Climates*. Fairbanks: Cold Climate Housing Research Center, 2014.

Tanaka, O. “An analysis of simultaneous heat and water vapor exchange through a flat paper plate crossflow total heat exchanger.” *International Journal of Heat and Mass Transfer* 27.12 (1984): 2259-2265.

Yoshino, M. Japan: Patent 47-19990. 1969.

Zhang, L.Z. “Heat and mass transfer in a cross-flow membrane-based enthalpy exchanger under naturally formed boundary conditions.” *International Journal of Heat and Mass Transfer 50* (2007): 151-162.

Zhang, L.Z., Cai, H.L., Pei, L.X. “Heat and moisture transfer in application scale parallel-plates enthalpy exchangers with novel membrane materials.” *Journal of Membrane Science 325* (2008): 672-682.

Zhang, L.Z., Jiang Y. “Heat and mass transfer in a membrane-based energy recovery ventilator.” *Journal of Membrane Science* 163 (1999): 29-38. <http://dx.doi.org/10.1016/S0376-7388(99)00150-7>.

Zhong, T.S., Li, Z.X., Zhang, L.Z. “Investigation of Membrane-Based Total Heat Exchangers with Different Structures and Materials.” *Journal of Membrane and Separation Technology* (2014): 1-10.

Aarnes, S.M. *Membrane Based Heat Exchanger*. Norway: NTNU, 2012.